Hydrology and
Earth System
Sciences
Discussions

Open Access

Investigating the impacts of biochar on water fluxes in tropical agriculture using stable isotopes

Benjamin M. C. Fischer[1,2,3], Laura Morillas[4], Johanna Rojas Conejo[5], Ricardo Sánchez-Murillo[6],

Andrea Suárez Serrano[5], Jay Frentress[7,8], Chih-Hsin Cheng[9], Monica Garcia[10], Stefano Manzoni[1,3],

Mark S. Johnson[11,12], and Steve W. Lyon[1,3,13]

[1] Department of Physical Geography, Stockholm University, Stockholm, Sweden.

[2] Department of Earth Sciences, Uppsala University, Uppsala, Sweden

[3] Bolin Centre for Climate Research, Stockholm University, Stockholm, Sweden

[4] Centre for Sustainable Food Systems, The University of British Columbia, Vancouver, British Columbia V6T 1Z4, Canada

[5] Water Resources Center for Central America and the Caribbean (HIDROCEC-UNA), Universidad Nacional de Costa Rica, Guanacaste,

[6] Stable Isotopes Research Group and Water Resources Management Laboratory, Universidad Nacional, Heredia, Costa Rica

[7] Free University of Bolzano, Italy

[8] Water Resources, Ramboll Sverige AB, Stockholm, Sweden

[9] School of Forestry and Resource Conservation, National Taiwan University, Taipei, Taiwan

[10] Department of Environmental Engineering, Technical University of Denmark, 2800 Kgs. Lyngby, Denmark

[11] Department of Earth, Ocean and Atmospheric Sciences, The University of British Columbia, Vancouver, British Columbia V6T 1Z4 Canada

[12] Institute for Resources, Environment and Sustainability, The University of British Columbia, Vancouver, British Columbia V6T 1Z4, Canada

[13] School of Environment and Natural Resources, Ohio State University, Ohio, USA

Correspondence to: B. M. C. Fischer (benjamin.fischer@natgeo.su.se)

Abstract

Amending soils with biochar, a pyrolyzed organic material, is an emerging practice to potentially increase plant available water. However, it is not clear (1) to what extent biochar amendments increase soil water storage relative to non-amended soils and (2) whether plants grown in biochar amended soils access different pools of water compared to those grown in non-amended soils. To investigate these questions, we set up an upland rice field experiment in a tropical seasonally dry region in Costa Rica, with plots treated with two different biochar amendments and control plots, from where we collected hydrometric and isotopic data ($\delta^{18}O$ and δ^2H from rain, soil, groundwater and rice plants). Our results show that the soil water retention curves for biochar treated soils shifted, indicating that rice plants had 2 % to 7 % more water available throughout the growing season relative to the control plots. In addition, we observed a within treatment variability in the soil water retention curves which was in the same order of magnitude as one would expect from responses due to differences in biochar application rates or due to differences in biochar typologies. The stable water isotope composition of plant water showed that the rice plants across all plots preferentially utilized the more variable soil water from the top 20 cm of the soil instead of using the deeper and less variable sources of water. Our results indicated that rice plants in biochar amended soils could access larger stores of water more consistently and thus could withstand dry spells of seven extra days relative to rice grown in non-treated soils. Though supplemental irrigation was required to facilitate plant growth during extended dry periods. Therefore, biochar amendments can complement, but not necessarily replace, other water management strategies.

1. Introduction

Rainfed agriculture provides food for the growing world population (Fraiture et al., 2009; Fraiture and Wichelns, 2010) without over-exploiting groundwater resources (Famiglietti, 2014; Jasechko et al., 2017). However, the spatial and temporal variability of rainfall makes rainfed agriculture vulnerable to droughts (Fischer et al., 2013) and poses a risk for food security (Fraiture and Wichelns, 2010). Extreme weather events such as El Niño-Southern Oscillation (ENSO) influence global precipitation patterns and can bring prolonged dry spells that limit rainfed agriculture production. This is especially true in the tropics, where rainfall regimes are changing and will continue to change (Feng et al., 2013; Giorgi, 2006; Knutson et al., 2006), leading to more frequent long-term droughts (i.e. periods of more than 10 years with limited rainfall; Hidalgo et al., 2019). Climate projections for the Mesoamerican tropics suggest (1) decreases in rainfall during the wet season (May-November) of 10 % to 25 %; (2) expansion of the areas affected by mid-summer droughts; and (3) increases in temperature and extreme dry spells – all of which result in a net decrease of water availability (Imbach et al., 2018). Such a decrease in water availability could have significant impacts on rainfed agricultural production and food security globally. Therefore, to reduce societal exposure to risk, it becomes necessary to make rainfed agriculture more resilient to current and future climate variability.

Agricultural innovations can offer a pathway forward. Common innovations considered capturing rain (Biazin et al., 2012) or flood water (Castelli et al., 2018), plant and soil water conservation measures (Enfors and Gordon, 2007; Makurira et al., 2007; Vico and Brunsell, 2018) or introducing supplementary irrigation (Mutiro et al., 2006). Amending soils with biochar is an emerging practice in agriculture that could be useful for improving resilience to climate variability (Fischer et al., 2018). Biochar is a collective name for organic material (e.g. woody or herbaceous vegetation, crop residues or waste material) that is pyrolyzed in low-tech (Sundberg et al., 2020) or high-tech furnaces (Liu et al., 2016). The result is a charcoal with different material properties (e.g. particle size, pore structure, surface area and hydrophobicity) from the original feedstock. Biochar can be applied on the soil surface or incorporated in the soil where it alters the original soil matrix thereby changing the infiltration capacity (Blanco-Canqui, 2017; Lim and Spokas, 2018; Sun and Lu, 2014) and creating a multilayer

Hydrology and
Earth System
Sciences
Discussions

Open Access

EGU

74   soil profile. The altered soil physical characteristics increase the soil water holding capacity and more

75   in general the amount of soil water stored at a given soil matric potential (Omondi et al., 2016).

76   However, despite documented positive effects of biochar amendments on agricultural productivity

77   (Kätterer et al., 2019; Novak et al., 2016), also negligible or no effects have also been observed (Fischer

78   et al., 2018; Jeffery et al., 2015, 2017; Nelissen et al., 2015; Reyes-Cabrera et al., 2017). These diverging

79   findings might be due to different biochar typologies (Fischer et al., 2018), but also to the fact that many

80   of the available studies are based on laboratory and pot experiments unable to mimic the variety of

81   processes occurring in agroecosystems at field scale (Agegnehu et al., 2017; Blanco-Canqui, 2017;

82   Zhang et al., 2016).

83   At the agroecosystem scale, soil water depends not only on the storage characteristics of the soil, but

84   also on variability of vertical fluxes resulting from rainfall and irrigation, evaporation, leakage and

85   runoff (Falkenmark, 1997; Rockström, 1999; Vico and Porporato, 2015). Thus, biochar impacts could

86   manifest themselves across the myriad pathways by which water can move through the soil-plant-

87   atmosphere continuum. Stable water isotopes can be a powerful tool to study how biochar additions

88   modify water stores and fluxes in agroecosystems. As part of the water molecule itself, the stable

89   isotopes of the water (^{18}O and ^{2}H) in combination with hydrometric data, are a proven tool to trace flow

90   pathways of water from rainfall (Fischer et al., 2017b) to evaporation (Benettin et al., 2018; Gonfiantini,

91   1986), through the (un)saturated zone (Jasechko et al., 2017; Koeniger et al., 2016; Sánchez-Murillo

92   and Birkel, 2016; Saxena, 1987), catchments (Fischer et al., 2017a; Klaus and McDonnell, 2013) and

93   more recently in the soil-plant-atmosphere continuum (Allen et al., 2019; Brooks et al., 2010; Dawson

94   and Ehleringer, 1991; McDonnell, 2014; Penna et al., 2018; Rothfuss and Javaux, 2017; Sprenger et

95   al., 2016).

96   Root water resembles the isotopic composition from the absorbed soil water from a specific location in

97   the soil profile (Berry et al., 2018), while, xylem water in the plant stem represents the isotopic

98   composition of all the soil profile within the root network (Dawson and Ehleringer, 1991; Penna et al.,

99   2018). To identify which water stores are available to vegetation, various potential water sources -e.g.,

100   rain (Fischer et al., 2019; Prechsl et al., 2014), soil water (Sprenger et al., 2015) and groundwater (Beyer

Hydrology and
Earth System
Sciences
Discussions

101 et al., 2016) are collected and analyzed for their stable isotope composition. The stable isotope

102 composition of the different collected water has allowed researchers to develop new theories whether

103 plants use soil-bound vs. mobile soil water pools (Brooks et al., 2010) or consume water from specific

104 soil layers that change over time (Berry et al., 2018; Beyer et al., 2016; Goldsmith et al., 2012; Koeniger

105 et al., 2016; Muñoz-Villers et al., 2020). Amin et al (2020) compared results from different stable

106 isotopes studies performed in natural catchments and deduced that plants in dry tropical climates

107 consume water from soil layers deeper than 50 cm. Beyond investigating natural ecosystems, stable

108 isotopes offer opportunities to study the sources of water in agroecosystems and quantifying the

109 efficiency of agricultural innovations.

110 Despite that stable isotopes have been used to a lesser extent in agricultural systems than in natural

111 systems to investigate plant water sources (Penna et al., 2020), there are successful studies done in

112 coffee (Muñoz-Villers et al., 2020), maize, wheat (Stumpp et al., 2009) and rice cultures

113 (Mahindawansha et al., 2018; Shen et al., 2015). In the case of rice, Shen et al. (2015) observed that

114 flooded rice consumed soil water from 0-15 cm deep, while Mahindawansha et al. (2018) found that

115 upland rice in dry conditions mostly consumed soil water from up to 50 cm deep except during the

116 maturing stage, when plants shifted to use water from the 10-30 cm soil depth. Based on this evidence,

117 we hypothesized that amending biochar into the top 10-30 cm of the soil, as it is commonly done, could

118 increase resilience to climate variability of upland rice in the tropics.

119 Our study seeks to test this hypothesis explicitly in a field experiment with upland rice in soil amended

120 with two different biochar types vs. a control treatment (no biochar) in a tropical seasonally dry region

121 in northwestern Costa Rica. We use a combination of hydrometric and isotopic data ($\delta^{18}O$ and $\delta^{2}H$ of

122 rain, soil, groundwater and rice plants) to target 1) to what extent do biochar amendments increase the

123 soil water storage relative to non-amended soils during the growing period of rice? and 2) do rice plants

124 grown in biochar amended soils access different pools of water compared to those grown in non-

125 amended soils?

2. Study site and experimental design

2.1 Study site

The biochar rice experiment was conducted at the Enrique Jímenez Núñez Experimental Station (EEEJN) from the Instituto Nacional de Innovación y Transferencia en Tecnología Agropecuaria (INTA) near the city of Cañas in the Guanacaste province of Costa Rica (Figure 1a). Soils at the experimental site are loamy vertosols (Table A1) typically more than 2 m deep (Diogenes Cubero and Maria José Elizondo, 2014). Guanacaste province is part of the Dry Corridor of Central America (Sánchez-Murillo et al., 2020) and characterized by a seasonally dry tropical climate with marked dry and wet seasons and limited temperature variability over a year (Birkel et al., 2017). The annual average temperature at EEEJN-INTA is 27.4 °C. The dry season typically spans from mid-November to April with virtually no rainfall. Wet season precipitation exhibits a bi-modal distribution dominated by the influence of the Intertropical Convergence Zone with peaks occurring in May/June and September/October. The moderate dry period between these two peaks is usually referred to as the mid-summer drought (Magaña et al., 1999). The average annual rainfall in the area is approximately 1,547 $\pm$ 473 mm yr^{-1} based on a 100-year observation record from a meteorological station ~10 km distance of the experimental site (Figure 2a). The annual average actual evapotranspiration is around 1,100 mm yr^{-1} (Sánchez-Murillo and Birkel, 2016). In the last century, 70 % of the driest years in this region (i.e., years with less than 1,153 mm yr^{-1} of rainfall, which is the 25th percentile of annual rainfall), occurred during warm ENSO years. Based on the Standardized Precipitation Index (SPI; Naresh Kumar et al., 2009), recurrent below average rainfall has been observed in this region since 1960s (Figure 2b) with a significant periodicity of severe (SPI<-1.5) and sustained droughts of around 10 years (Hidalgo et al., 2019).

2.2 Experimental design

For this experiment two types of biochar were tested to represent a more locally-produced biochar and a more industrially-processed biochar, respectively. Biochar 1 (BC1) was made of locally sourced bamboo (*Guadua angustifolia*) and produced at the Costa Rica Institute of Technology (TEC, Cartago, CR; Table A1). The feedstock consisted of wood pieces up to 30 cm in length from construction waste, which were pyrolyzed using a pyrolysis furnace under a temperature ranging 450-480 °C. A second

154   biochar, biochar 2 (BC2) was produced from sugarcane filter cake collected from the Huwei Sugar Mill

155   (Taiwan Sugar Corporation, Taipei, Taiwan). For the industrial processing of BC2, the filter cake was

156   pelletized into pellets with 7.6 mm diameter and 20-30 mm long and pyrolyzed at 600 °C under a

157   controlled nitrogen-rich atmosphere. Pyrolyzed pellets were crushed and sieved to ≤ 2 mm prior to field

158   application.

159   Within the EEEJN-INTA experimental station, an area of approximately 160 m^2 was delineated and

160   divided into three sections of 40 m^2 each for treatments. The three different treatment sections, one for

161   each biochar type (BC1 and BC2) and a control treatment (C) with no biochar added, were subdivided

162   into three plots each to create three independent monitoring replicates of each treatment (Figure 1b).

163   The BC1 and C plots were 7 m^2 each (5 m long x 1.4 m wide) in area while the BC2 plots were 3.5 m^2

164   each (2.5 m long x 1.4 m wide) in area. This difference in areas between biochar treatments was due to

165   a lower amount of BC2 being available (shortage of feedstock at the biochar supplier) while securing a

166   similar application rate (1 kg m^{-2}) across biochar treatments. For the biochar treatments, the ≤ 2 mm

167   particle size biochar was mechanically worked into the top 20 cm of the field prior to planting. It should

168   be noted that BC1 was incorporated into the field about six months earlier than BC2 due to logistical

169   constraints. BC1 addition was followed by an irrigated melon crop on the treated plot prior to our rice

170   experiment.

171   After the treatment sections were prepared, an upland rice variety Palmar 18 (*Oryza sativa* L.) was sown

172   simultaneously on the three sections on 18 July 2018 indicating the start of the experiment. For sowing,

173   5 cm deep longitudinal rills were created in all plots with a spacing of 25 cm. In each rill, rice seeds

174   were sown by hand of about 1 seed cm^{-1}, equivalent to 20 g m^{-2}. After sowing, the rills were covered

175   with soil. During the growing season, rice plants were primarily rainfed which is the standard procedure

176   for the predominant upland rice grown in the region. In some cases, where water sources for irrigation

177   are available, sporadic support irrigation is used by local farmers to support crops and avoid wither.

178   Due to prolonged dry spells that occurred during the study period, all experimental plots were irrigated

179   with 7 L m^{-2} on July 22 and August 25 to assist germination and avoid plant drought damage

180   respectively on each date. Following typical regional crop management practices, fertilizer (100 g m^{-2}

181   consisting of 10 % N, 30 % P, 10 % K in combination of 11 ml MEGAFOL® and 11 g magnesium

182   sulphate) and insecticide/herbicide (2 ml Muralla® Delta; 50 ml Garlon and 20 ml bispiribac sodium)

183   were applied to all experimental plots using 2 L m^{-2} irrigation water on each treatment date (August 10,

184   September 6, and November 5) to support plant growth. At monthly intervals, manual weed control was

185   performed in all plots. Harvest took place on 21 November 2018 and indicated the end of the

186   experiment.

187   ## 2.3 Instrumentation and sampling

188   ### 2.3.1 Meteorological and hydrometric observations

189   A meteorological station (Vaisala WT520; 1.5 m height) was used to continuously monitor

190   precipitation, wind speed and direction, air temperature, relative humidity and atmospheric pressure at

191   the site during the entire study period (Figure 1b and c). Each experimental plot was instrumented with

192   one sensor installed at 15 cm depth to monitor volumetric soil water content, soil electrical conductivity

193   and soil temperature (model GS3, Decagon Devices, Inc., Pullman USA), and one additional sensor at

194   same depth to monitor soil matric potential and soil temperature (model MPS6, Decagon Devices). Both

195   sensors were between rice rows in each plot (Figure 1c). Additionally, soil samples were collected at

196   15 cm soil depth from each plot at the beginning of the experiment and after harvest to determine the

197   gravimetric soil moisture content. These data were used to perform a two-point calibration of the

198   volumetric soil water content measurements derived from the sensors at each plot during the entire time

199   series.

200   Depth of groundwater levels was measured using a groundwater well (groundwater well A) installed

201   between the BC1 and C treatment sections (Figure 1b). The well consisted of screened PVC tube

202   instrumented with a sensor to continuously monitor groundwater level, electrical conductivity and water

203   temperature (model CTD, Decagon Devices). Manual water level measurements were also made every

204   other week during the study period to calibrate the continuous sensor data. All sensors were connected

205   to a datalogger (Campbell CR1000 logger and an AM416 Relay Multiplexer) and programmed to record

206   at 30-minute intervals.

Hydrology and
Earth System
Sciences
Open Access
Discussions
EGU

2.3.2 Water and plant sample collection

Water samples from different pools of water (namely, rainwater, irrigation water, soil water and groundwater) were collected for isotopic analysis. Rainwater was collected using a funnel connected with tubing to a PET bottle (1.5 liter) wrapped in aluminum foil similar to Prechsl et al. (2014). In each plot, lysimeters (Soilmoisture equipment corp., Santa Barbara, USA) were installed in the soil reaching to 15 cm and 40 cm soil depth respectively to sample soil water. Groundwater samples were collected from a second groundwater well (groundwater well B) installed near the BC2 treatment section (Figure 1b).

Rainwater samples were collected daily at 7:00 AM. Water from additional application sources such as irrigation (to supplement rainfall) and fertilizer/pesticide/herbicide applications were sampled as a grab sample using a PE bottle during each application. Soil water and groundwater samples were collected approximately biweekly (every other week) after plant germination from 31 July 2018 until the harvest day on 21 November 2018, resulting in 11 sampling days. Soil water was collected from lysimeters by applying an 800-mbar vacuum for 2 minutes. Groundwater was sampled by purging the well and waiting 1 hour before collecting the groundwater sample. All water samples were collected in 30 ml PE bottles, which were capped and sealed with Parafilm® for transport and cold storage (5 °C) until analysis. At the end of each sampling day, all excess water from all sampler tubing, bottles, and suction lysimeters was removed to prevent inter-sampling contamination.

Plant material from the rice plants was also collected on each of the 11 biweekly sampling dates at around 12:00 noon. For plant material sampling, six rice plants were randomly selected within each plot. The plant height from the soil to the plant tip was measured and recorded before sampling. To avoid loss of biomass on sampled plants, the plants were extracted using a small knife which was carefully wiggled into the soil. The roots, stems and leaves of the extracted plants were separated immediately and transferred into double re-sealable zipper storage bag. To minimize post-sampling transpiration, storage bags were directly placed in a cooler with ice. All plant material was stored in the laboratory freezer (-80 °C) before extracting the plant water for isotopic analysis.

Hydrology and
Earth System
Sciences
Discussions
Open Access

EGU

3. Laboratory methods and data analysis

3.1 Plant water extraction

Plant water was extracted from the stem (xylem water) of the different rice plants to infer which sources of water the rice plants used. We used the cryogenic vacuum extraction technique described by Koeniger et al., (2011) to extract the plant water for stable isotope analysis. The method uses a heated vial and a cold trap vial (Exetainer® vial with standard cap and rubber septum, Labco Ltd, Lampeter, United Kingdom) connected with stainless-steel capillary tubing. About 3 g of plant material from the rice stem was placed in the heated vial before the system was evacuated to 85 kPa with a vacuum hand pump (Mityvac). The heated vial was heated for 1 hour at 100°C using a test tube heater (HI839800 COD Test Tube Heater; Hanna instruments) while the cold trap vial rested in a Dewar flask containing liquid nitrogen at about -196°C. After the extraction was stopped, the cold trap vial was sealed with Parafilm and left to thaw. After thawing, the extracted liquid water was pipetted into 2 ml vials (32 x 11.6 mm screw neck vials with cap and PTFE/silicone/PTFE septa) and stored cold (5 °C) until stable isotope analysis. On average 86±5 % plant water was extracted from xylem.

3.2 Isotope analysis

All non-plant water samples were filtered (0.45 μm filter 13 mm PTFE Syringe Filter, Fisher scientific) and pipetted in vials (2 mL into a 1.5 mL 32 × 11.6 mm screw neck vials with cap and PTFE/silicone/PTFE septa) prior to analysis. Water stable isotopes analysis was conducted at the Stable Isotopes Research Group facilities of the Universidad Nacional of Costa Rica using a water isotope analyzer LWIA-45P (Los Gatos Research Inc., USA). All data were normalized and corrected for drift and memory effects. The analytical long-term error was $\pm$ 0.5 (‰) (1σ) for δ^2H and $\pm$ 0.1 (‰) (1σ) for $\delta^{18}O$.

Plant water stable isotopes analysis was conducted at the Swedish University of Agricultural Sciences (SLU) Stable Isotope Laboratory (SSIL) in Umeå using an Isotope Ratio Mass Spectrometer (TC/EA-IRMS; DeltaV Advantage, Thermo Fisher Scientific, Bremen, Germany; High Temperature Conversion Elemental Analyzer, Thermo Fisher Scientific, Bremen, Germany and an AI 1310 Autosampler, Thermo Fisher Scientific, Bremen, Germany). All water samples were injected into a glassy carbon

260   reactor containing glassy carbon chips at 1,400°C and converted to H_2 and CO gases which were

261   separated on a column and analyzed on a mass spectrometer. All data were corrected for drift and

262   memory. The analytical precision and accuracy were ± 2 (‰) (1σ) for δ^2H and ± 0.15 (‰) (1σ) for

263    $\delta^{18}O$.

264   All stable isotope compositions are presented as delta notations (δ) in ‰, relating the ratios (R) of

265    $^{18}O/^{16}O$ and $^2H/^1H$, relative to the VSMOW-SLAP scale. The Global Meteoric Water Line (GMWL)

266   was defined as $\delta^2H = 8 \cdot \delta^{18}O + 10$ by Craig (1961). The Local Meteoric Water Line (LMWL) was derived

267   as $\delta^2H = 7.4 \cdot \delta^{18}O + 5.5$ using the long term isotopic data from the rain sampler at the Water Resources

268   Center for Central America and the Caribbean (Sánchez-Murillo et al., in review) located ~50 km

269   distance of the experimental site. In addition, the deuterium excess (d-excess) was defined as d-excess

270    $= \delta^2H - 8 \cdot \delta^{18}O$ (Dansgaard, 1964).

271   3.3 Evapotranspiration and soil water retention impacts

272   Daily evapotranspiration rates (ET) from the experimental area were estimated by the crop coefficient

273   method ($ET = K_c \cdot ET_{ref}$) or FAO56 Penman-Monteith method (Allen et al., 1998). We used site specific

274   meteorological observations to estimate daily reference ET (ET_{ref}) and experimentally derived crop

275   coefficient (K_c) values for the three different stages of the crop growth (initial, mid-season, and late-

276   season). Instead of using globally averaged values of K_c for rice (Allen et al., 1998), we used region-

277   specific K_c values experimentally derived from a nearby field experimental site equipped with an Eddy

278   Covariance (EC) tower where the same variety of upland rice is grown (Morillas et al., 2019). Daily K_c

279   values from the EC site where derived as the ratio of daily measured ET and site-specific ET_{ref}, and then

280   averaged for the three stationary crop growth stages (K_c initial = 0.7, K_c mid-season = 0.9 and K_c late

281   season = 0.5). The length of each crop growth stage was also calibrated for this region by observing the

282   pattern of daily measured ET over the whole growing season (initial ≈ 25 days, development ≈ 20 days,

283   mid-season ≈ 50 days, late-season ≈ 23 days for an average growing season of 120 days).

284   Field derived 30-minute records of all meteorological and hydrometric observations (precipitation,

285   volumetric soil water content, soil matric potential and groundwater level) were aggregated to daily

286   averages. Accumulated precipitation and evapotranspiration were also derived from daily

Hydrology and
Earth System
Sciences
Discussions

Open Access

EGU

287   measurements and estimates respectively for the entire experimental period (July 18-November 21).

288   Average volumetric soil water content and soil matric potential for each treatment (BC1, BC2 and C)

289   were calculated by averaging the observations in the three replicated plots per treatment.

290   Treatment specific volumetric soil water content (θ) and soil matric potential (ψ) were linked through

291   soil water retention curves using the Van Genuchten model (Van Genuchten, 1980) (Eq. 1)

$$\theta = \theta_r + \frac{\theta_s - \theta_r}{[1 + (\alpha\,\psi)^n]^m} \qquad (1)$$

292   where θ_r [%], α [-] and n [-] represent residual, and the fitted scale and shape parameters, respectively;

293   parameter and $m = 1 - 1/n$ [-] while saturation soil moisture (θ_s) is based on field observations. To

294   examine the effect of biochar on soil physical and hydraulic properties, we compared the indicators θ_{WP};

295   θ_{FC} and van Genuchten parameter α and n estimated for the biochar amended treatments (BC1 and

296   BC2) with the same indicators for the unamended treatment (C) using response ratios (RR) as in Fischer

297   et al. (2018). For this study, RR represents the ratio of the variable of interest in the treatment to the

298   same property in the control such that $RR>1$ or R<1 indicates that the treatment has a positive or

299   respectively negative effect.

300   3.4 Plant water source estimation

301   The isotopic composition of the water samples was represented in the dual isotope space $\delta^{18}O$ and δ^2H

302   to infer which sources of water rice plants consumed. To represent a potential plant water source under

303   rainfed conditions, the isotope composition of rainfall was considered as the volume weighted isotope

304   composition of rainfall collected in the two-week period before a given plant water sampling day. Since

305   residual rainfall can evaporate while in the soil (simplified assumption not accounting of mixing with

306   pre-event water), the isotopic composition of the residual rainfall for each water sampling day was

307   estimated following (Gonfiantini, 1986) and (Benettin et al., 2018)

$$\delta_{PR} = (\delta_P - \delta^*)(1 - f_E)^U + \delta^* \qquad (2)$$

308   where δ_{PR} [‰], δ_P [‰], and f_E [-] represent the isotopic compositions of the residual rainfall, the

309   volume weighted isotope composition of rainfall collected in the two-week period before a sampling

Hydrology and
Earth System
Sciences
Discussions
Open Access
EGU

310   day, and the fraction of rainfall that fell in the two-week period before a sampling day and that has

311   evaporated on the sampling day, respectively. The variables δ^*[‰] and U [-] represents the limiting

312   isotopic composition and the temporal enrichment slope, which were determined using equation 3 and

313   4 respectively

$$\delta^* = \frac{R_H \delta_A + \varepsilon_k + \dfrac{\varepsilon^+}{\alpha^+}}{R_H - 10^{-3}\left(\varepsilon_k + \dfrac{\varepsilon^+}{\alpha^+}\right)} \tag{3}$$

$$U = \frac{R_H - 10^{-3}\left(\varepsilon_k + \dfrac{\varepsilon^+}{\alpha^+}\right)}{1 - R_H \varepsilon_k} \tag{4}$$

314   where R_H[-] represents the average relative humidity of the two-week period before a sampling day, δ_A

315   [‰] the approximation of the isotopic composition of the atmospheric vapor (equation 5 following

316   Gibson et al., (2016)), ε_k [‰] the simplified kinetic fractionation factor (Eq. 6) and ε^+ [‰] and α^+ [-] the

317   two equilibrium fractionation factors (Eq. 7 and 8).

$$\delta_A = \frac{\delta_P - \varepsilon^+}{\alpha^+} \tag{5}$$

$$\varepsilon_k = (1 - R_H)(1 - S_{18O \ or \ 2H})10^3 \tag{6}$$

$$10^3 \ln(\alpha^+\delta\ ^2H)$$
$$= 1158.8\frac{T^3}{10^9} - 1620.1\frac{T^2}{10^6} + 794.84\frac{T}{10^3} - 161.04$$
$$+ 2.9992\frac{10^9}{T^3}$$

or $\tag{7}$

$$10^3 \ln(\alpha^+\delta^{18}O) = 0.3504\frac{10^9}{T^3} - 1.6664\frac{10^6}{T^2} + 6.7123\frac{10^3}{T} - 7.685$$

$$\varepsilon^+ = (\alpha^+ - 1)10^3 \tag{8}$$

318   where $S_{18O} = 0.9755$ and $S_{2H} = 0.9723$ (Merlivat, 1978) and T [K] represents the average

319   temperature of the two-week period before a sampling day. The volume-weighted isotope composition

320   of rainfall before each sampling day, which was generally near the GMWL and LMWL, and the

321   corresponding estimated isotopic composition of the residual rainfall, which was generally off the

322   GMWL and LMWL, provided the start and end point of a theoretical evaporation line in dual isotope

323   space. Similarly, an evaporation line for the median sampled soil water of a period was developed. Such

324   evaporation lines map the evolution of the soil water available from residual rainfall or evaporated soil

325   water for plants to be consumed between sampling days allowing us to track which stores of water the

326   rice plants interact with across the treatments. In addition, the within treatment variability defined as

327   difference between the minimum and maximum observed isotopic composition of plant water within a

328   treatment on any given sampling day were calculated.

329   # 4. Results

330   ## 4.1 Hydrometric variability

331   Based on the temporal variability of rainfall, we identified three distinct periods within the overall study

332   period (Figure 3). Period I (18 July to 20 September) was characterized with alternating wet and dry

333   days, Period II (20 September to 9 November) presented consistent high daily rainfall inputs, and Period

334   III (10 November to 21 November) was characterized by a long dry spell ending with rice harvest.

335   Throughout the study period, daytime air temperatures were around 26.7 °C (standard deviation = 3 °C)

336   and evapotranspiration rates on average 3.1 mm day^{-1} (standard deviation = 0.7 mm day^{-1}).

337   During Period I (germination and vegetative phase), the rice in the different plots grew to a height of

338   50 cm in all experimental plots (standard deviation <2.5 cm). This period was characterized by

339   intermittent dry and wet spells with accumulated precipitation slightly higher than evapotranspiration

340   (P_{cum}= 240 mm and ET_{cum}= 191 mm over the 64-day period; Figure 3b). During this period, the

341   maximum recorded volumetric soil water contents were 40 %, 43 %, and 35 %, and decreased to the

342   minimum values 30 %, 25 %, and 23 % in the BC1, BC2, and control treatment, respectively (Figure

343   3c). Regarding soil matric potential (ψ) during this period, it surpassed field capacity (ψ_{FC} = -0.05

344   MPa) with a maximum of -0.008 MPa during rain events and decreased to a minimum of -0.32 MPa

345   observed in all treatments a few days after the third sampling day as a result of the driest spell of Period

346   I (Figure 3d). Generally, the soil matric potential in the biochar treatments was 0.002 MPa higher than

347   in the control treatment and never reached the wilting point (ψ_{WP} = -1.5 MPa). The groundwater level

348   was generally 0.7 m below the surface, rising after sampling day 1 to less than 0.6 m below the surface

349   before sampling day 4, and to less than 0.5 m below the surface in response to the largest rainfall of

350   Period I (Figure 3e).

351   During Period II (vegetative and reproductive phase), rice plants attained their maximum heights of

352   around 100 cm (standard deviation <5 cm), across all three plots (Period II was the wettest period with

353   15 out of 42 rain days with intensities greater than 20 mm d^{-1} of rainfall (and one day with 93 mm d^{-1})

354   (Figure 3a and b). This wet condition lead to cumulative precipitation being much greater than

355   cumulative evapotranspiration during the period (P$_{cum}$= 570 mm and ET$_{cum}$= 147 mm; over the 50-day

356   period). The volumetric soil water content over Period II was generally higher than in Period I, with

357   multiple peaks driven by rainfall events and then a decrease towards the end of the period. After rain

358   events, the volumetric soil water contents rose from 28 % to 40 %, from 24 % to 45 %, and from 23 %

359   to 36 % in BC1, BC2, and control treatment, respectively. Soil moisture then decreased in the three

360   treatments to 32 %, 38 %, and 32 % during the last part of the period. The soil matric potential during

361   Period II remained largely above field capacity except by the end of the period when it decreased (before

362   sampling day 8) to a minimum of -0.23 MPa in BC1 and -0.16 MPa in BC2 and C. The groundwater

363   level increased multiple times during this period from 0.7 m below the surface to reach the soil surface

364   the rainiest day of the study period. Between Sampling days 6 and 7, groundwater level remained no

365   lower than 0.4 m below the surface.

366   During the final experimental period, Period III (ripening phase), rice plants maintained their maximum

367   height acquired by the end of Period II. This period was characterized by a 12 day long dry spell such

368   that cumulative evapotranspiration was greater than cumulative precipitation (P$_{cum}$= 2 mm and ET$_{cum}$=

369   63 mm; 12-day period). By the end of Period III, the volumetric soil water content in the BC1 and BC2

370   treatments converged to the lowest observed value of ~21 %. It is relevant that the control treatment

371   reached this value about seven days earlier than the biochar amended plots, and the control plots

372 continued decreasing to reach a minimum value of 18 % (Figure 3c). The soil matric potential for all

373 three plots decreased from above the field capacity to near the wilting point by the end of Period III.

374 The groundwater level also decreased from 0.4 m to 0.8 m below the surface (i.e. the sampling well

375 went dry).

376 ## 4.2 Impact of biochar on soil water retention curves

377 The soil water retention curves from the different treatments showed different shapes and different

378 volumetric water content at a given soil matric potential (Figure 4). Comparing the different soil water

379 retention curves across the different plots of the different treatments shows a within treatment

380 variability, i.e., range of different volumetric soil moisture contents relative to the observed soil matric

381 potentials (Figure 4). Comparing the different soil water retention curves across the periods shows that

382 biochar treatments increased volumetric soil moisture content relative to the control treatment

383 consistently across the ranges of observed soil matric potentials in all three periods (Figure 4, Table

384 A2). The soil water retention curves estimated for Period III were shifted to lower volumetric water

385 contents relative to the other periods and ranged from close to field capacity to wilting point.

386 The effect of biochar on the soil water retention curve can also be quantified by the response ratios of

387 the wilting point, field capacity and the van Genuchten parameters α and n. Most of these ratios were

388 found to be larger than one (Table 1), which indicates increased soil water content for a given water

389 potential value.

390 ## 4.3 Isotopic variability

391 Overall, the $\delta^{18}O$ and d-excess of rainfall was between -15.7 ‰ and -0.2 ‰ (S_D = 3.4 ‰) and 0 ‰ and

392 +18 ‰ (S_D = 4.6 ‰) respectively ($\delta^{18}O$ see Figure 5a, d-excess see Figure A2a and A3). The $\delta^{18}O$ and

393 d-excess of soil water and groundwater collected on the different sampling days was between -7.5 ‰

394 and -4.5 ‰ (S_D = 1.3 ‰) and -1.1 ‰ and +9.7 ‰ (S_D = 4.9 ‰) respectively ($\delta^{18}O$ see Figure 5b-d, d-

395 excess see Figure A2b-d and A3). The within treatment variability in isotopic composition of soil water

396 samples for each sample day was <1 ‰ for $\delta^{18}O$ and <6 ‰ for d-excess (Figure 6). The $\delta^{18}O$ and d-

397 excess of plant water was between -8.7 ‰ and -2.7 ‰ (S_D = 3.7 ‰) and -14.6 ‰ to +3.2 ‰ (S_D = 11.4

398 ‰) respectively ($\delta^{18}O$ see Figure 5b-d, d-excess see Figure A2b-d and A3). The within treatment

399   variability in isotopic composition of plant water samples on each sample day >3 ‰ for δ^{18}O and >8 ‰

400   for d-excess (Figure 6). The within treatment variability was smaller for the biochar amended treatments

401   relative to the within treatment variability in the control treatment (Figure 6).

402   During Period I, the isotopic composition of rainfall varied between -5.6 ‰ to -0.2 ‰ for δ^{18}O (Figure

403   5a) and from -1.1 ‰ to +9 ‰ for d-excess (Figure A2). On rainy days when rainfall intensities were

404   below 10 mm d^{-1}, sub-cloud evaporation may exert an important control on rainfall enrichment

405   (Sánchez-Murillo et al., 2016, 2017) and potentially also the low amount of rain water collected in

406   relation to the bottle volume causing water to evaporated water in the sampler. For example, the

407   observed fractionated isotopic compositions of these rain samples were often recorded to be <5 ‰ with

408   regard to d-excess. The average isotopic composition of plant water in the different treatments decreased

409   from roughly from +3.2 ‰ to -4 ‰ for δ^{18}O and increased from roughly -40 ‰ to +18 ‰ for d-excess

410   during Period I (Figures 5 and A2). In Period II, the isotopic composition of rainfall varied between -

411   3.7 ‰ to -12.7 ‰ for δ^{18}O (Figure 5a) and +6 ‰ to +11.8 ‰ for d-excess (Figure A2). The average

412   isotopic composition of plant water varied in all treatments to between -7 ‰ to -2 ‰ for δ^{18}O and -11.8

413   ‰ to +9.2 ‰ for d-excess. It should be noted that there was a change from negative to positive d-excess

414   for the plant water isotopic compositions between sampling day five and seven, indicating a change

415   from highly fractionated isotopic compositions to compositions similar to that of rainfall. During the

416   dry spell of Period III no rainfall occurred and hence no rainwater was collected. Also, no soil water

417   could be extracted from lysimeters sampling water from 15 below the surface on sampling day 10 and

418   day 11. The average isotopic composition of plant water varied between -7 ‰ to -6 ‰ for δ^{18}O and -7

419   ‰ to -2 ‰ for d-excess, showing a high fractionation signature (Figures 5, A2 and A3).

420   ## 4.4 Using dual isotope space to characterize plant water sources

421   Rainfall isotopic compositions fell along the GMWL and LMWL for our experimental site (Figure 7).

422   The soil water and ground water isotopic samples from Period I were more fractionated, i.e. they

423   deviated from the GMWL, compared to soil water isotopic samples from the wet Period II and III which

424   fell more along the GMWL (Figure 8). The plant water isotopic compositions from the different

425   treatments and sampling periods were somewhat different from each other in terms of absolute values

426   but showed a similar temporal evolution (Figure 7). In Period I, plant water samples from all treatments

427   deviated from the GMWL and moved primarily along the modeled evaporation lines of the sampled

428   soil water (Figure 7 a, d and g). The plant water thus resembled soil water with a strong evaporation

429   signature in Period I.

430   In Period II, which was much wetter than Period I, the plant water samples fell on or were close to the

431   GMWL independent of the treatment and moved from sampling day to sampling day along the GMWL.

432   It is likely that plant water responded to the replenished soil water that acquired the signature of rainfall

433   during this period. At the end of Period II, plant water samples from BC1 and the control treatment

434   showed a more fractioned signature and fell on the modelled evaporation line indicating that plant water

435   resembled soil water with signature from evaporated rain from day 8 (Figure 7 b and h). Plant water

436   samples in the BC2 treatment, however, showed the signature from soil water more similar to original

437   rainfall (Figure 7 e and e2). During the dry Period III, all plant water samples deviated from the GMWL

438   and fell along modeled evaporation lines with signature of residual rainfall that had fallen in Period II

439   (depicted in blue in Figure 7 c, f, and i).

5. Discussion

440

5.1 Variable effect of biochar on the soil hydraulic properties

441

442   Incorporating two different types of biochar in plots planted with rice affected the soil hydraulic

443   properties. The soil water retention curves of the biochar amended treatments showed higher soil water

444   contents at similar matric potential relative to the control treatment, leading to more plant water

445   available under similar conditions (Figure 4, Table 1). The soil water retention curve of the BC1

446   treatment became more similar to the curves found in finer grained soils, which indicates increased

447   water retention, a common expected impact of biochar additions (Fischer et al., 2018; Sun and Lu,

448   2014). Conversely, the soil water retention curve for the BC2 treatment became more similar to the

449   curves associated with coarser soils indicating enhanced water flows, which has also been described as

450   a potential impact of biochar additions (Fischer et al., 2018; Liu et al., 2017).

451   The overall soil response to biochar amendments in our experiment had a within treatment variability

452   but was comparable to the response found in other tropical soils where a lower range of θ_{WP} and θ_{FC}

Hydrology and
Earth System
Sciences
Discussions
EGU
Open Access

453   was found (Obia et al., 2016). But the soil water retention curves we found were more irregular shaped

454   compared to laboratory derived soil water retention curves reported in the literature (Iiyama, 2016;

455   Morgan et al., 2001) which usually present one single continuous drying curve (e.g. Batool et al., 2015;

456   Głąb et al., 2016 or Obia et al., 2016). Instead the field-data derived soil water retention curves in the

457   present study were field derived and the result of temporally variable atmospheric forcing. Specifically,

458   our observed within treatment variability in the soil water retention curves was a same order of

459   magnitude as the responses due to differences in biochar application rates or due to differences in

460   biochar typologies reported in laboratory studies (e.g. Batool et al., 2015; Głąb et al., 2016 or Obia et

461   al., 2016). Laboratory studies may overestimate the volumetric soil moisture content at a given soil

462   matric potential compared to field-derived soil water retention curves (Iiyama, 2016; Morgan et al.,

463   2001).

464   Although the two biochar types tested were produced in different ways, their experimental application

465   was similar (i.e. same application rate, similar particle size, application amount, depth, site

466   characteristics and climate). One key distinction between the two biochar treatments was the application

467   date, which may be important because aging can change the physical and chemical characteristics of

468   biochar (Blanco-Canqui, 2017). Due to some logistical constraints, biochar was introduced to the BC1

469   plot about six months before the BC2 plot. This allowed the biochar to age in situ and for the disturbed

470   soils to settle under the BC1 treatment. Thus, the BC2 soil likely had relatively larger macropores that

471   could have increased the connectivity of the 20 cm soil layer where biochar was applied with deeper

472   soil layers. This difference in application timing may have influenced the hydraulic differences in

473   results observed between the two biochar treatments (Figure 4) and amplified the differences due to the

474   contrasting production methods. Clearly, the interplay of all the possible biochar variables with all the

475   possible site-specific heterogeneities makes it challenging to isolate the biochar effect in

476   agroecosystems. Taken altogether, these differences in biochar treatment responses and the relative

477   impacts of both B1 and B2 biochar treatments compared to the control plot highlights the potential for

478   variability in biochar responses – which has been documented in the literature (Fischer et al., 2018) and

479   creates ambiguity around predicting the response of biochar amendments at field scale. This further

480   highlighting the difficulty to transfer laboratory-scale results to the field scale where management

481   decisions are made.

482   5.2 Temporally variable soil water fluxes

483   The isotopic composition of different water samples was useful to infer how water fluxes varied through

484   time. The isotopic composition of soil water sampled at two different depths across the plots was rather

485   stable over time compared to the temporally variable isotopic composition of rainfall (Figure 5). In

486   addition, the temporal variability of isotopic composition of soil water from our experiment was less

487   than the spatial variability or change in isotopic composition with depth reported in previous biochar

488   studies (e.g. Beyer et al., 2016; Koeniger et al., 2016; Saxena, 1987 and Sprenger et al., 2016). When

489   comparing our findings with other tropical systems, the d-excess of the soil water we found during dry

490   spells (Figure A2) had a smaller variation range than observed in a coffee plantation in Mexico by

491   Muñoz-Villers et al. (2020) and was generally less variable than observations made by Jiménez-

492   Rodríguez et al. (2020) in a tropical wet forest in Costa Rica. The low d-excess values and ranges of

493   the soil water observed in this study indicate high evaporative processes in the top soil layer (Amin et

494   al., 2020; Sprenger et al., 2016). This is consistent with our high estimated evapotranspiration rates

495   (average 3.1 mm day^{-1} up to 6 mm day^{-1}) which are typical for the Dry Corridor of Central America

496   characterized by high solar radiation and air temperatures (Morillas et al., 2019).

497   During Period I, when rice plants were small and sparse, leaving much bare soil, the evaporation

498   occurring from the soil across the different treatments was homogenous, creating a low d-excess signal

499   in the soil water. During wet spells in Period II, the d-excess increased slightly, indicating mixing of

500   rainfall with soil water. At the end of Period II and throughout Period III, the d-excess remained higher

501   despite high evaporation, which might be due to a more homogenous crop cover creating a consistent

502   microclimate as described by Sprenger et al. (2017). The isotopic composition of groundwater (1) had

503   d-excess values similar to that of meteoric water during dry spells and (2) decreased during wet spells

504   showing a high evaporative signal (Figure A2). Such observed changes in d-excess are generally not

505   found in temperate zones (Sprenger et al., 2016), but indicate that rainfall flushed the fractionated soil

506   water downwards promoting mixing with groundwater (Gat and Airey (2006).

5.3 Temporally variable plant water sources

507

508   The studied rice plants had different water sources available during different periods of the experiment,

509   but what water did they consume?

510   It is likely that the fractionation observed in the plant water collected in this study represents fractioned

511   soil water that was consumed by the plants. This is consistent with results observed in previous studies

512   using stable water isotopes to map out plant water sources (Brooks et al., 2010; Penna et al., 2020;

513   Sprenger et al., 2016). Further, this interpretation of plant water composition is supported by plant water

514   samples falling along the theoretical evaporation lines estimating how soil water would evolves

515   isotopically due to evaporation. Therefore, it is likely that during Period I, the young rice plants (with

516   shallow root system <20 cm as reported by Mahindawansha et al. 2018) consumed the fractionated soil

517   water (Figure 7) which was not sampled with the lysimeters at 15 cm and 40 cm below the surface.

518   During Period II, plants grew to their maximum heights with roots reaching deeper soil layers (length

519   >60 cm as reported by Mahindawansha et al. 2018). This means that the rice plants, similar to larger

520   vegetation e.g. trees (Allen et al., 2019), would have had access to deeper and more-stable pools of

521   water with a distinct lower d-excess signature. However, the isotopic composition of plant water during

522   this period followed the GMWL (Figure 7 b, e and h), indicating that plants consumed largely shallow

523   soil water from recent rainfall. In Period III, it became increasingly difficult to extract water from

524   lysimeters at 15 cm below the surface and the isotopic composition of plant water drifted from the

525   GMWL, along the theoretical evaporation line of residual rainfall which fell in Period II. With the

526   experiment being held in the tropics and based on Amin et al (2020) one would expect that the rice

527   plants with their longer roots would accessed access the more stable and older water stores in deeper

528   subsurface zones below 60 cm. Instead, the rice plants in the different treatments preferably consumed

529   the temporally variable and isotopically labeled newer surface soil water similarly to what has been

530   documented in natural ecosystems (e.g. van der Velde et al., 2015) and temperate grasslands (Bachmann

531   et al., 2015).

532   By mixing biochar in the top soil, a multi-layer soil profile was created and based on studies in natural

533   catchments, e.g. Penna et al. (2018) or Sprenger et al. (2016), these different layers could store not only

534   different quantities of water but also water characterized by different ages. Performing additional

535   isotopic experiments (Beyer et al., 2016), higher temporal resolution sampling of plant water (Marshall

536   et al., 2020; Volkmann et al., 2016) and spatiotemporal soil water (Sprenger et al., 2015) or including

537   interception, transpiration and atmospheric processes into the experimental analysis (Jiménez-

538   Rodríguez et al., 2020) would allow to not only distinguish in more detail whether the rice plants prefer

539   bounded or mobile water (Berry et al., 2018; Brooks et al., 2010; McDonnell, 2014) but also to quantify

540   the fraction of water sources (Muñoz-Villers et al., 2020). Consequently, this would also allow to

541   indicate how long the soil water resides in the different soil layers before it is consumed by plants. In

542   addition to the aforementioned vertical processes also the lateral water fluxes (Sprenger and Allen,

543   2020) need to be considered to assess the field-scale responses to biochar amendments (Fischer et al.,

544   2018). These analyses are beyond the scope of this initial investigation; however, our results indicate

545   that rice plants growing in biochar amended soils not only had access to more water (Figure 4) but also

546   had a more stable source of green water (i.e. soil moisture from rainfall) and thus could withstand dry

547   spells seven days longer (Figure 3). Regardless of the potential advantages, as stated by Fischer et al.

548   (2018), it must be noted that biochar as water management tool does not adhere to a one size fits all

549   approach but needs fine tuning in accordance with climate, site and plant characteristics to obtain stable

550   and optimal yields.

6. Conclusions

552   Amending soils with biochar is an emerging and promising practice to improving resilience of rainfed

553   agriculture to climate variability by increasing the soil water and plant available water. Using an

554   experimental field study, we observed biochar amendments to create generally 2 % to 7 % higher soil

555   water content and therefore more plant water relative to the control treatment, despite differing impacts

556   between biochar treatments depending on the type of biochar and timing of application. In addition, we

557   observed a within treatment variability in the soil water retention curves which was in the same order

558   of magnitude as one would expect from responses due to differences in biochar application rates or due

559   to differences in biochar typologies. Further, we were able to trace the effect of biochar on the soil water

560   storage to investigate which water plants consume. The isotopic composition of soil water sampled in

Hydrology and
Earth System
Sciences
Discussions

Open Access

EGU

561 two distinct depths in the different plots was rather stable in time compared to the temporal variable

562 isotopic composition of rainfall. The stable isotope composition of plant water instead showed that the

563 rice plants preferably consumed the temporal variable soil water comprised of residual rainfall the

564 experienced evaporation in the top 20 cm of the soil. When comparing the different treatments, our

565 results indicated that rice plants grown in biochar amended soils not only had more water available but

566 also had a more stable source of green water. Thus, these rice plants in biochar amended soils could

567 withstand dry spells of up to an extra seven days. Despite these positive effects of biochar amendment,

568 it still seems necessary to provide additional irrigation to facilitate optimal plant growth if extended dry

569 periods occur during certain growing stages to have optimal yields. So, while our study highlights some

570 of the usefulness of combining hydrometric and isotopic data to map out how biochar additions impact

571 plant-water interactions in the field, we acknowledge more work is needed to fully characterize the

572 influence biochar additions may have at scale on agroecosystems. This further understanding is

573 important given the need of more specific management recommendations to ensure biochar additions

574 in agricultural landscapes result in net benefits for both farmers and the environment.

Data availability

576 Upon acceptance, all of the research data that were required to create the plots will be available from

577 the Bolin Center for Climate Research.

Author contribution

579 BF, LM, MG, SM, MJ, AS and SL designed the experiment, and BF, JR carried it out. CC provided

580 BC2, RS analyzed the stable isotope composition of the collected water. BF performed the data analysis

581 and prepared the paper with contributions from all co-authors.

Competing interests

583 The authors declare that they have no conflict of interest.

Acknowledgements

593   ## Financial support

References

604

605 Agegnehu, G., Srivastava, A. K. and Bird, M. I.: The role of biochar and biochar-compost in improving
606   soil quality and crop performance: A review, Applied Soil Ecology, 119, 156–170,
607   doi:10.1016/j.apsoil.2017.06.008, 2017.

608 Allen, R. G., Pereira, L. S., Raes, D. and Smith, M.: Crop evapotranspiration-Guidelines for computing
609   crop water requirements, FAO, Rome., 1998.

610 Allen, S. T., Kirchner, J. W., Braun, S., Siegwolf, R. T. W. and Goldsmith, G. R.: Seasonal origins of
611   soil water used by trees, Hydrol. Earth Syst. Sci., 23(2), 1199–1210, doi:10.5194/hess-23-1199-
612   2019, 2019.

613 Amin, A., Zuecco, G., Geris, J., Schwendenmann, L., McDonnell, J. J., Borga, M. and Penna, D.: Depth
614   distribution of soil water sourced by plants at the global scale: A new direct inference approach,
615   Ecohydrology, 13(2), e2177, doi:10.1002/eco.2177, 2020.

616 Bachmann, D., Gockele, A., Ravenek, J. M., Roscher, C., Strecker, T., Weigelt, A. and Buchmann, N.:
617   No Evidence of Complementary Water Use along a Plant Species Richness Gradient in
618   Temperate Experimental Grasslands, PLOS ONE, 10(1), 1–14,
619   doi:10.1371/journal.pone.0116367, 2015.

620 Batool, A., Taj, S., Rashid, A., Khalid, A., Qadeer, S., Saleem, A. R. and Ghufran, M. A.: Potential of
621   soil amendments (Biochar and Gypsum) in increasing water use efficiency of Abelmoschus
622   esculentus L. Moench, Frontiers in Plant Science, 6(September), 1–13,
623   doi:10.3389/fpls.2015.00733, 2015.

624 Benettin, P., Volkmann, T. H. M., von Freyberg, J., Frentress, J., Penna, D., Dawson, T. E. and
625   Kirchner, J. W.: Effects of climatic seasonality on the isotopic composition of evaporating soil
626   waters, Hydrology and Earth System Sciences, 22(5), 2881–2890, doi:10.5194/hess-22-2881-
627   2018, 2018.

628 Berry, Z. C., Evaristo, J., Moore, G., Poca, M., Steppe, K., Verrot, L., Asbjornsen, H., Borma, L. S.,
629   Bretfeld, M., Hervé-Fernández, P., Seyfried, M., Schwendenmann, L., Sinacore, K., De
630   Wispelaere, L. and McDonnell, J.: The two water worlds hypothesis: Addressing multiple
631   working hypotheses and proposing a way forward, Ecohydrology, 11(3), e1843,
632   doi:10.1002/eco.1843, 2018.

633 Beyer, M., Koeniger, P., Gaj, M., Hamutoko, J. T., Wanke, H. and Himmelsbach, T.: A deuterium-
634   based labeling technique for the investigation of rooting depths, water uptake dynamics and
635   unsaturated zone water transport in semiarid environments, Journal of Hydrology, 533, 627–
636   643, doi:10.1016/j.jhydrol.2015.12.037, 2016.

637 Biazin, B., Sterk, G., Temesgen, M., Abdulkedir, A. and Stroosnijder, L.: Rainwater harvesting and
638   management in rainfed agricultural systems in sub-Saharan Africa – A review, Physics and
639   Chemistry of the Earth, Parts A/B/C, 47–48, 139–151, doi:10.1016/j.pce.2011.08.015, 2012.

640 Birkel, C., Brenes, A. and Sánchez-Murillo, R.: The Tempisque-Bebedero catchment system: energy-
641   water-food consensus in the seasonally dry tropics of northwestern Costa Rica, in Nexus
642   Outlook: assessing resource use challenges in the water, energy and food nexus, TH-Koeln,
643   University of Applied Sciences. [online] Available from: https://www.water-energy-

644   food.org/fileadmin/user_upload/files/documents/others/Outlook-
645   Nexus_Assessing_Resource_Use_Challenges.pdf, 2017.

646 Blanco-Canqui, H.: Biochar and Soil Physical Properties, Soil Science Society of America Journal,
647   81(4), 687, doi:10.2136/sssaj2017.01.0017, 2017.

648 Brooks, R. J., Barnard, H. R., Coulombe, R. and McDonnell, J. J.: Ecohydrologic separation of water
649   between trees and streams in a Mediterranean climate, Nature Geoscience, 3(2), 100–104,
650   doi:10.1038/ngeo722, 2010.

651 Castelli, G., Bresci, E., Castelli, F., Hagos, E. Y. and Mehari, A.: A participatory design approach for
652   modernization of spate irrigation systems, Agricultural Water Management, 210, 286–295, doi:
653   10.1016/j.agwat.2018.08.030, 2018.

654 Craig, H.: Isotopic Variations in Meteoric Waters, Science, 133(3465), 1702–1703,
655   doi:10.1126/science.133.3465.1702, 1961.

656 Dansgaard, W.: Stable isotopes in precipitation, Tellus, 16(4), 436–468, doi:10.1111/j.2153-
657   3490.1964.tb00181.x, 1964.

658 Dawson, T. E. and Ehleringer, J. R.: Streamside trees that do not use stream water, Nature, 350(6316),
659   335–337, doi:10.1038/350335a0, 1991.

660 Diogenes Cubero, F. and Maria José Elizondo, A.: Estudio detallado de suelos y capacidad de uso de
661   las tierras de estación experimental enrique jiménez núñez (Detailed study of soils and capacity
662   of use of the lands of experimental station enrique jiménez núñez), Instituto Nacional de
663   Innovación y Transferencia en Tecnología Agropecuaria, Cañas., 2014.

664 Enfors, E. I. I. and Gordon, L. J. J.: Analysing resilience in dryland agro-ecosystems: a case study of
665   the Makanya catchment in Tanzania over the past 50 years, Land Degradation & Development,
666   18(6), 680–696, doi:10.1002/ldr.807, 2007.

667 Falkenmark, M.: Society's interaction with the water cycle: a conceptual framework for a more holistic
668   approach, Hydrological Sciences Journal, 42(4), 451–466, doi:10.1080/02626669709492046,
669   1997.

670 Famiglietti, J. S.: The global groundwater crisis, Nature Climate Change, 4(11), 945–948,
671   doi:10.1038/nclimate2425, 2014.

672 Feng, X., Porporato, A. and Rodriguez-Iturbe, I.: Changes in rainfall seasonality in the tropics, Nature
673   Climate Change, 3(9), 811–815, doi:10.1038/nclimate1907, 2013.

674 Fischer, B. M. C., Mul, M. L. and Savenije, H. H. G.: Determining spatial variability of dry spells: a
675   Markov-based method, applied to the Makanya catchment, Tanzania, Hydrology and Earth
676   System Sciences, 17(6), 2161–2170, doi:10.5194/hess-17-2161-2013, 2013.

677 Fischer, B. M. C., Stähli, M. and Seibert, J.: Pre-event water contributions to runoff events of different
678   magnitude in pre-alpine headwaters, Hydrology Research, 48(1), 28–47,
679   doi:10.2166/nh.2016.176, 2017a.

680 Fischer, B. M. C., van Meerveld, H. J. (Ilja) and Seibert, J.: Spatial variability in the isotopic
681   composition of rainfall in a small headwater catchment and its effect on hydrograph separation,
682   Journal of Hydrology, 547, 755–769, doi:10.1016/j.jhydrol.2017.01.045, 2017b.

683 Fischer, B. M. C., Manzoni, S., Morillas, L., Garcia, M., Johnson, M. S. and Lyon, S. W.: Improving
684   agricultural water use efficiency with biochar – A synthesis of biochar effects on water storage
685   and fluxes across scales, Science of The Total Environment, doi:
686   10.1016/j.scitotenv.2018.11.312, 2018.

687 Fischer, B. M. C., Aemisegger, F., Graf, P., Sodemann, H. and Seibert, J.: Assessing the Sampling
688   Quality of a Low-Tech Low-Budget Volume-Based Rainfall Sampler for Stable Isotope
689   Analysis, Frontiers in Earth Science, 7, 244, doi:10.3389/feart.2019.00244, 2019.

690 Fraiture, C. de and Wichelns, D.: Satisfying future water demands for agriculture, Agricultural Water
691   Management, 97(4), 502–511, doi: 10.1016/j.agwat.2009.08.008, 2010.

692 Fraiture, C. de, Karlberg, L. and Rockström, J.: Can rainfed agriculture feed the world? An assessment
693   of potentials and risk, in Rainfed agriculture: Unlocking the potential., pp. 124–132, CAB
694   International, London., 2009.

695 Gat, J. R. and Airey, P. L.: Stable water isotopes in the atmosphere/biosphere/lithosphere interface:
696   Scaling-up from the local to continental scale, under humid and dry conditions, Global and
697   Planetary Change, 51(1), 25–33, doi:10.1016/j.gloplacha.2005.12.004, 2006.

698 Gibson, J. J., Birks, S. J. and Yi, Y.: Stable isotope mass balance of lakes: a contemporary perspective,
699   Quaternary Science Reviews, 131, 316–328, doi:10.1016/j.quascirev.2015.04.013, 2016.

700 Giorgi, F.: Climate change hot-spots, Geophysical Research Letters, 33(8),
701   doi:10.1029/2006GL025734, 2006.

702 Głąb, T., Palmowska, J., Zaleski, T. and Gondek, K.: Effect of biochar application on soil hydrological
703   properties and physical quality of sandy soil, Geoderma, 281, 11–20,
704   doi:10.1016/j.geoderma.2016.06.028, 2016.

705 Goldsmith, G. R., Muñoz-Villers, L. E., Holwerda, F., McDonnell, J. J., Asbjornsen, H. and Dawson,
706   T. E.: Stable isotopes reveal linkages among ecohydrological processes in a seasonally dry
707   tropical montane cloud forest, Ecohydrology, 5(6), 779–790, doi:10.1002/eco.268, 2012.

708 Gonfiantini, R.: Chapter 3 - environmental isotopes in lake studies, in The Terrestrial Environment, B,
709   edited by P. Fritz and J. C. Fontes, pp. 113–168, Elsevier, Amsterdam., 1986.

710 Hidalgo, H. G., Alfaro, E. J., Amador, J. A. and Bastidas, Á.: Precursors of quasi-decadal dry-spells in
711   the Central America Dry Corridor, Climate Dynamics, 53(3), 1307–1322, doi:10.1007/s00382-
712   019-04638-y, 2019.

713 Iiyama, I.: Differences between field-monitored and laboratory-measured soil moisture characteristics,
714   Soil Science and Plant Nutrition, 62(5–6), 416–422, doi:10.1080/00380768.2016.1242367,
715   2016.

716 Imbach, P., Chou, S. C., Lyra, A., Rodrigues, D., Rodriguez, D., Latinovic, D., Siqueira, G., Silva, A.,
717   Garofolo, L. and Georgiou, S.: Future climate change scenarios in Central America at high
718   spatial resolution, PLOS ONE, 13(4), e0193570, doi:10.1371/journal.pone.0193570, 2018.

719 Jasechko, S., Perrone, D., Befus, K. M., Bayani Cardenas, M., Ferguson, G., Gleeson, T., Luijendijk,
720   E., McDonnell, J. J., Taylor, R. G., Wada, Y. and Kirchner, J. W.: Global aquifers dominated
721   by fossil groundwaters but wells vulnerable to modern contamination, Nature Geoscience,
722   10(6), 425–429, doi:10.1038/ngeo2943, 2017.

723 Jeffery, S., Meinders, M. B. J., Stoof, C. R., Bezemer, T. M., van de Voorde, T. F. J., Mommer, L. and
724   van Groenigen, J. W.: Biochar application does not improve the soil hydrological function of a
725   sandy soil, Geoderma, 251–252, 47–54, doi:10.1016/j.geoderma.2015.03.022, 2015.

726 Jeffery, S., Abalos, D., Prodana, M., Bastos, A. C., Van Groenigen, J. W., Hungate, B. A. and Verheijen,
727   F.: Biochar boosts tropical but not temperate crop yields, Environmental Research Letters,
728   12(5), doi:10.1088/1748-9326/aa67bd, 2017.

729 Jiménez-Rodríguez, C. D., Coenders-Gerrits, M., Wenninger, J., Gonzalez-Angarita, A. and Savenije,
730   H.: Contribution of understory evaporation in a tropical wet forest during the dry season,
731   Hydrol. Earth Syst. Sci., 24(4), 2179–2206, doi:10.5194/hess-24-2179-2020, 2020.

732 Kätterer, T., Roobroeck, D., Andrén, O., Kimutai, G., Karltun, E., Kirchmann, H., Nyberg, G.,
733   Vanlauwe, B. and Röing de Nowina, K.: Biochar addition persistently increased soil fertility
734   and yields in maize-soybean rotations over 10 years in sub-humid regions of Kenya, Field Crops
735   Research, 235, 18–26, doi:10.1016/j.fcr.2019.02.015, 2019.

736 Klaus, J. and McDonnell, J. J.: Hydrograph separation using stable isotopes: Review and evaluation,
737   Journal of Hydrology, 505, 47–64, doi:10.1016/j.jhydrol.2013.09.006, 2013.

738 Knutson, T. R., Delworth, T. L., Dixon, K. W., Held, I. M., Lu, J., Ramaswamy, V., Schwarzkopf, M.
739   D., Stenchikov, G. and Stouffer, R. J.: Assessment of Twentieth-Century Regional Surface
740   Temperature Trends Using the GFDL CM2 Coupled Models, J. Climate, 19(9), 1624–1651,
741   doi:10.1175/JCLI3709.1, 2006.

742 Koeniger, P., Marshall, J. D., Link, T. and Mulch, A.: An inexpensive, fast, and reliable method for
743   vacuum extraction of soil and plant water for stable isotope analyses by mass spectrometry,
744   Rapid Communications in Mass Spectrometry, 25(20), 3041–3048, doi:10.1002/rcm.5198,
745   2011.

746 Koeniger, P., Gaj, M., Beyer, M. and Himmelsbach, T.: Review on soil water isotope-based
747   groundwater recharge estimations, Hydrological Processes, 30(16), 2817–2834,
748   doi:10.1002/hyp.10775, 2016.

749 Lim, T.-J. and Spokas, K.: Impact of Biochar Particle Shape and Size on Saturated Hydraulic Properties
750   of Soil, Korean Journal of Environmental Agriculture, 37(1), 1–8, doi:KJEA-37-1, 2018.

751 Liu, C., Wang, H., Tang, X., Guan, Z., Reid, B. J., Rajapaksha, A. U., Ok, Y. S. and Sun, H.: Biochar
752   increased water holding capacity but accelerated organic carbon leaching from a sloping
753   farmland soil in China, Environmental Science and Pollution Research, 23(2), 995–1006,
754   doi:10.1007/s11356-015-4885-9, 2016.

755 Liu, Z., Dugan, B., Masiello, C. A. and Gonnermann, H. M.: Biochar particle size, shape, and porosity
756   act together to influence soil water properties, PLOS ONE, 12(6), 1–19,
757   doi:10.1371/journal.pone.0179079, 2017.

758 Magaña, V., Amador, J. A. and Medina, S.: The Midsummer Drought over Mexico and Central
759   America, J. Climate, 12(6), 1577–1588, doi:10.1175/1520-
760   0442(1999)012<1577:TMDOMA>2.0.CO;2, 1999.

761 Mahindawansha, A., Orlowski, N., Kraft, P., Rothfuss, Y., Racela, H. and Breuer, L.: Quantification of
762   plant water uptake by water stable isotopes in rice paddy systems, Plant and Soil, 429(1), 281–
763   302, doi:10.1007/s11104-018-3693-7, 2018.

764   Makurira, H., Mul, M. L., Vyagusa, N. F., Uhlenbrook, S. and Savenije, H. H. G.: Evaluation of
765   community-driven smallholder irrigation in dryland South Pare Mountains, Tanzania: A case
766   study of Manoo micro dam, Physics and Chemistry of the Earth, Parts A/B/C, 32(15–18), 1090–
767   1097, doi: 10.1016/j.pce.2007.07.020, 2007.

768   Marshall, J., Cuntz, M., Beyer, M., Dubbert, M. and Kuehnhammer, K.: Borehole Equilibration: Testing
769   a New Method to Monitor the Isotopic Composition of Tree Xylem Water in situ, Frontiers in
770   Plant Science, 11, doi:10.3389/fpls.2020.00358, 2020.

771   McDonnell, J. J.: The two water worlds hypothesis: ecohydrological separation of water between
772   streams and trees?, WIREs Water, 1(4), 323–329, doi:10.1002/wat2.1027, 2014.

773   Merlivat, L.: Molecular diffusivities of H2 16O, HD16O, and H2 18O in gases, J. Chem. Phys., 69(6),
774   2864–2871, doi:10.1063/1.436884, 1978.

775   Morgan, K. T., Parsons, L. R. and Adair Wheaton, T.: Comparison of laboratory- and field-derived soil
776   water retention curves for a fine sand soil using tensiometric, resistance and capacitance
777   methods, Plant and Soil, 234(2), 153–157, doi:10.1023/A:1017915114685, 2001.

778   Morillas, L., Hund, S. V. and Johnson, M. S.: Water Use Dynamics in Double Cropping of Rainfed
779   Upland Rice and Irrigated Melons Produced Under Drought-Prone Tropical Conditions, Water
780   Resources Research, 55(5), 4110–4127, doi:10.1029/2018WR023757, 2019.

781   Muñoz-Villers, L. E., Geris, J., Alvarado-Barrientos, M. S., Holwerda, F. and Dawson, T.: Coffee and
782   shade trees show complementary use of soil water in a traditional agroforestry ecosystem,
783   Hydrology and Earth System Sciences, 24(4), 1649–1668, doi:10.5194/hess-24-1649-2020,
784   2020.

785   Mutiro, J., Makurira, H., Senzanje, A. and Mul, M. L.: Water productivity analysis for smallholder
786   rainfed systems: A case study of Makanya catchment, Tanzania, Physics and Chemistry of the
787   Earth, Parts A/B/C, 31(15–16), 901–909, doi:10.1016/j.pce.2006.08.019, 2006.

788   Narseh Kumar, M., Murthy, C. S., Sesha Sai, M. V. R. and Roy, P. S.: On the use of Standardized
789   Precipitation Index (SPI) for drought intensity assessment, Meteorological Applications, 16(3),
790   381–389, doi:10.1002/met.136, 2009.

791   Nelissen, V., Ruysschaert, G., Manka Abusi, D., D' Hose, T., De Beuf, K., Al-Barri, B., Cornelis, W.
792   and Boeckx, P.: Impact of a woody biochar on properties of a sandy loam soil and spring barley
793   during a two-year field experiment, European Journal of Agronomy, 62, 65–78,
794   doi:10.1016/j.eja.2014.09.006, 2015.

795   Novak, J., Ro, K., Ok, Y. S., Sigua, G., Spokas, K., Uchimiya, S. and Bolan, N.: Biochars
796   multifunctional role as a novel technology in the agricultural, environmental, and industrial
797   sectors, Chemosphere, 142, 1–3, doi:10.1016/j.chemosphere.2015.06.066, 2016.

798   Obia, A., Mulder, J., Martinsen, V., Cornelissen, G. and Børresen, T.: In situ effects of biochar on
799   aggregation, water retention and porosity in light-textured tropical soils, Soil and Tillage
800   Research, 155, 35–44, doi:10.1016/j.still.2015.08.002, 2016.

801   Omondi, M. O., Xia, X., Nahayo, A., Liu, X., Korai, P. K. and Pan, G.: Quantification of biochar effects
802   on soil hydrological properties using meta-analysis of literature data, Geoderma, 274, 28–34,
803   doi:10.1016/j.geoderma.2016.03.029, 2016.

Hydrology and
Earth System
Sciences
Discussions

804   Penna, D., Hopp, L., Scandellari, F., Allen, S. T., Benettin, P., Beyer, M., Geris, J., Klaus, J., Marshall,
805   J. D., Schwendenmann, L., Volkmann, T. H. M., von Freyberg, J., Amin, A., Ceperley, N.,
806   Engel, M., Frentress, J., Giambastiani, Y., McDonnell, J. J., Zuecco, G., Llorens, P., Siegwolf,
807   R. T. W., Dawson, T. E. and Kirchner, J. W.: Ideas and perspectives: Tracing terrestrial
808   ecosystem water fluxes using hydrogen and oxygen stable isotopes – challenges and
809   opportunities from an interdisciplinary perspective, Biogeosciences, 15(21), 6399–6415,
810   doi:10.5194/bg-15-6399-2018, 2018.

811   Penna, D., Geris, J., Hopp, L. and Scandellari, F.: Water sources for root water uptake: Using stable
812   isotopes of hydrogen and oxygen as a research tool in agricultural and agroforestry systems,
813   Agriculture, Ecosystems & Environment, 291, 106790, doi:10.1016/j.agee.2019.106790, 2020.

814   Prechsl, U. E., Gilgen, A. K., Kahmen, A. and Buchmann, N.: Reliability and quality of water isotope
815   data collected with a low-budget rain collector, Rapid Communications in Mass Spectrometry,
816   28(8), 879–885, doi:10.1002/rcm.6852, 2014.

817   Reyes-Cabrera, J., Erickson, J. E., Leon, R. G., Silveira, M. L., Rowland, D. L., Sollenberger, L. E. and
818   Morgan, K. T.: Converting bahiagrass pasture land to elephantgrass bioenergy production
819   enhances biomass yield and water quality, Agriculture, Ecosystems and Environment,
820   248(July), 20–28, doi:10.1016/j.agee.2017.07.021, 2017.

821   Rockström, J.: On-farm green water estimates as a tool for increased food production in water scarce
822   regions, Physics and Chemistry of the Earth, Part B: Hydrology, Oceans and Atmosphere,
823   24(4), 375–383, doi:10.1016/S1464-1909(99)00016-7, 1999.

824   Rothfuss, Y. and Javaux, M.: Reviews and syntheses: Isotopic approaches to quantify root water uptake:
825   a review and comparison of methods, Biogeosciences, 14(8), 2199–2224, doi:10.5194/bg-14-
826   2199-2017, 2017.

827   Sánchez-Murillo, R. and Birkel, C.: Groundwater recharge mechanisms inferred from isoscapes in a
828   complex tropical mountainous region, Geophysical Research Letters, 43(10), 5060–5069,
829   doi:10.1002/2016GL068888, 2016.

830   Sánchez-Murillo, R., Esquivel-Hernándezv, G., Birkel, C., Correa, A., Welsh, K., Durán-Quesada, A.
831   M., Sánchez-Gutiérrez, R. and Poca, M.: Tracing water sources and fluxes in a dynamic tropical
832   environment: from observations to modelingv, Frontiers in Earth Science, in review.

833   Sánchez-Murillo, R., Birkel, C., Welsh, K., Esquivel-Hernández, G., Corrales-Salazar, J., Boll, J.,
834   Brooks, E., Roupsard, O., Sáenz-Rosales, O., Katchan, I., Arce-Mesén, R., Soulsby, C. and
835   Araguás-Araguás, L. J.: Key drivers controlling stable isotope variations in daily precipitation
836   of Costa Rica: Caribbean Sea versus Eastern Pacific Ocean moisture sources, Quaternary
837   Science Reviews, 131, 250–261, doi:10.1016/j.quascirev.2015.08.028, 2016.

838   Sánchez-Murillo, R., Durán-Quesada, A. M., Birkel, C., Esquivel-Hernández, G. and Boll, J.: Tropical
839   precipitation anomalies and d-excess evolution during El Niño 2014-16, Hydrological
840   Processes, 31(4), 956–967, doi:10.1002/hyp.11088, 2017.

841   Sánchez-Murillo, R., Esquivel-Hernández, G., Corrales-Salazar, J. L., Castro-Chacón, L., Durán-
842   Quesada, A. M., Guerrero-Hernández, M., Delgado, V., Barberena, J., Montenegro-Rayo, K.,
843   Calderón, H., Chevez, C., Peña-Paz, T., García-Santos, S., Ortiz-Roque, P., Alvarado-Callejas,
844   Y., Benegas, L., Hernández-Antonio, A., Matamoros-Ortega, M., Ortega, L. and Terzer-

845   Wassmuth, S.: Tracer hydrology of the data-scarce and heterogeneous Central American
846   Isthmus, Hydrological Processes, 34(11), 2660–2675, doi:10.1002/hyp.13758, 2020.

847   Saxena, R.: Oxygen-18 fractionation in nature and estimation of groundwater recharge [Rayleigh
848   distillation formula, reverse Rayleigh process, throughfall], Report-University of Uppsala,
849   Department of Physical Geography, Hydrological Division Series A (Sweden), 1987.

850   Shen, Y. J., Zhang, Z. B., Gao, L. and Peng, X.: Evaluating contribution of soil water to paddy rice by
851   stable isotopes of hydrogen and oxygen, Paddy and Water Environment, 13(1), 125–133,
852   doi:10.1007/s10333-013-0414-y, 2015.

853   Sprenger, M. and Allen, S. T.: What Ecohydrologic Separation Is and Where We Can Go With It, Water
854   Resources Research, 56(7), e2020WR027238, doi:10.1029/2020WR027238, 2020.

855   Sprenger, M., Herbstritt, B. and Weiler, M.: Established methods and new opportunities for pore water
856   stable isotope analysis, Hydrological Processes, 29(25), 5174–5192, doi:10.1002/hyp.10643,
857   2015.

858   Sprenger, M., Leistert, H., Gimbel, K. and Weiler, M.: Illuminating hydrological processes at the soil-
859   vegetation-atmosphere interface with water stable isotopes, Reviews of Geophysics, 54(3),
860   674–704, doi:10.1002/2015RG000515, 2016.

861   Sprenger, M., Tetzlaff, D. and Soulsby, C.: Soil water stable isotopes reveal evaporation dynamics at
862   the soil–plant–atmosphere interface of the critical zone, Hydrol. Earth Syst. Sci., 21(7), 3839–
863   3858, doi:10.5194/hess-21-3839-2017, 2017.

864   Stumpp, C., Maloszewski, P., Stichler, W. and Fank, J.: Environmental isotope (δ18O) and hydrological
865   data to assess water flow in unsaturated soils planted with different crops: Case study lysimeter
866   station   "Wagna"   (Austria),   Journal   of   Hydrology,   369(1),   198–208,
867   doi:10.1016/j.jhydrol.2009.02.047, 2009.

868   Sun, F. and Lu, S.: Biochars improve aggregate stability, water retention, and pore-space properties of
869   clayey   soil,   Journal   of   Plant   Nutrition   and   Soil   Science,   177(1),   26–33,
870   doi:10.1002/jpln.201200639, 2014.

871   Sundberg, C., Karltun, E., Gitau, J. K., Kätterer, T., Kimutai, G. M., Mahmoud, Y., Njenga, M., Nyberg,
872   G., Roing de Nowina, K., Roobroeck, D. and Sieber, P.: Biochar from cookstoves reduces
873   greenhouse gas emissions from smallholder farms in Africa, Mitigation and Adaptation
874   Strategies for Global Change, doi:10.1007/s11027-020-09920-7, 2020.

875   Van Genuchten, M. T.: A closed-form equation for predicting the hydraulic conductivity of unsaturated
876   soils, Soil science society of America journal, 44(5), 892–898, 1980.

877   van der Velde, Y., Heidbüchel, I., Lyon, S. W., Nyberg, L., Rodhe, A., Bishop, K. and Troch, P. A.:
878   Consequences of mixing assumptions for time-variable travel time distributions: Mixing
879   assumptions and time-variable travel time distributions, Hydrological Processes, 29(16), 3460–
880   3474, doi:10.1002/hyp.10372, 2015.

881   Vico, G. and Brunsell, N. A.: Tradeoffs between water requirements and yield stability in annual vs.
882   perennial   crops,   Advances   in   Water   Resources,   112,   189–202,   doi:
883   10.1016/j.advwatres.2017.12.014, 2018.

884   Vico, G. and Porporato, A.: Ecohydrology of Agroecosystems: Quantitative Approaches Towards
885   Sustainable Irrigation, Bulletin of Mathematical Biology, 77(2), 298–318, doi:10.1007/s11538-
886   014-9988-9, 2015.

887   Volkmann, T. H. M., Kühnhammer, K., Herbstritt, B., Gessler, A. and Weiler, M.: A method for in situ
888   monitoring of the isotope composition of tree xylem water using laser spectroscopy, Plant, Cell
889   & Environment, 39(9), 2055–2063, doi:10.1111/pce.12725, 2016.

890   Zhang, D., Yan, M., Niu, Y., Liu, X., van Zwieten, L., Chen, D., Bian, R., Cheng, K., Li, L., Joseph,
891   S., Zheng, J., Zhang, X., Zheng, J., Crowley, D., Filley, T. R. and Pan, G.: Is current biochar
892   research addressing global soil constraints for sustainable agriculture?, Agriculture, Ecosystems
893   & Environment, 226, 25–32, doi:10.1016/j.agee.2016.04.010, 2016.

894 Table

895 **Table 1** **Response ratios for wilting point (θ_{WP}), minimum observed average volumetric soil moisture contents (θ_{min}) field**
896 **capacity (θ_{FC}), and for the van Genuchten parameters α and n (Equation 1) for BC1 and BC2. Parameters are**
897 **derived for the average soil water retention curve of figure 4 for Periods I-III. A response ratio RR > 1 indicates**
898 **that biochar has a positive effect on a soil water content while a RR ≈ 1 indicates that biochar has no effect,**
899 **while RR < 1 indicates a negative response for the variable of interest.**

	BC	Period I	Period II	Period III
$\theta_{WP\ BC}\ \theta_{WP\ C}^{-1}$	1	1.36	1.46	1.18
	2	1.16	1.32	1.03
$\theta_{min\ BC}\ \theta_{min\ C}^{-1}$	1	1.12	1.16	1.17
	2	1.08	1.03	1.11
$\theta_{FC\ BC}\ \theta_{FC\ C}^{-1}$	1	1.08	1.14	1.04
	2	1.13	1.13	0.88
$\alpha_{BC}\ \alpha_{C}^{-1}$	1	1.29	0.50	0.68
	2	3.21	1.34	1.08
$n_{BC}\ n_{C}^{-1}$	1	1.00	0.89	1.47
	2	1.00	0.92	1.06

900

901 Figures
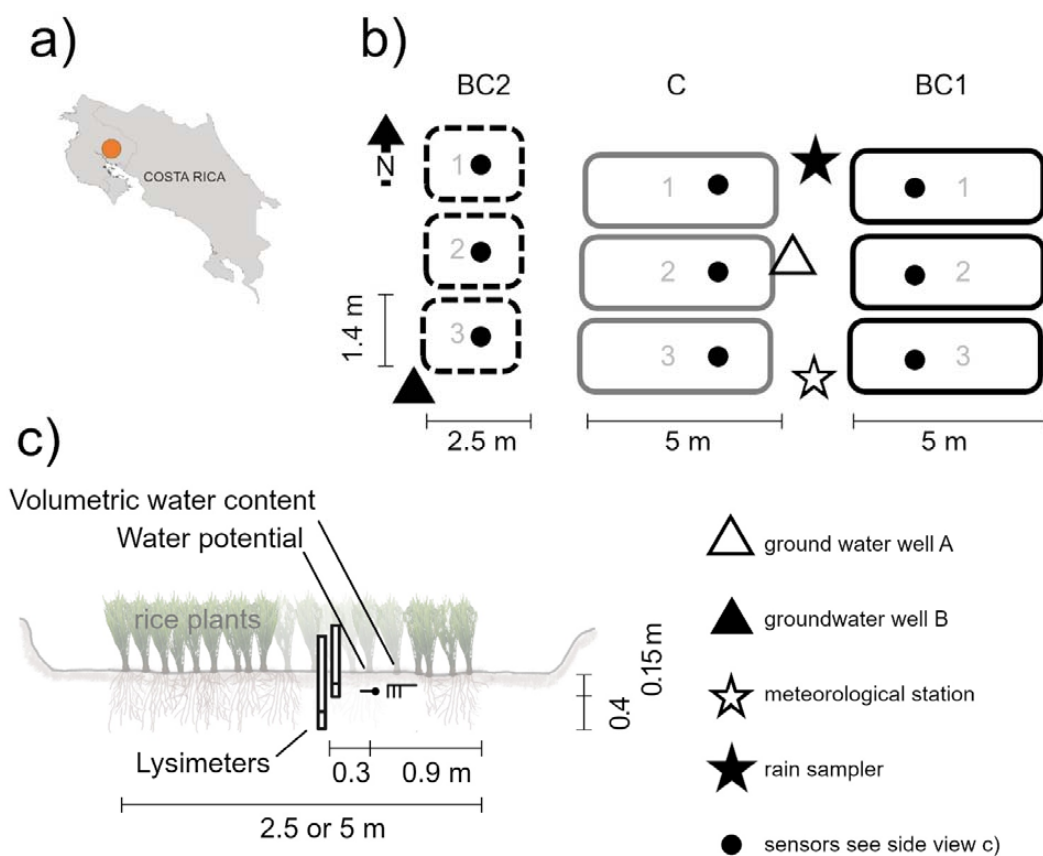
902

903 **Figure 1** *(a) Map of Costa Rica with location of the experimental site (orange circle), (b) schematic top view of the rice*
904 *experiment with the three different treatment sections, BC1, BC2 and C. Symbols indicate the different*
905 *instruments: rain sampler for stable isotope samples (filled star), meteorological station (open star), continues*
906 *groundwater level measurements in well A (open triangle), groundwater well B for stable isotope samples*
907 *(closed triangle) and (c) a schematic side view of a plot with suction lysimeters for stable isotope samples 15 cm*
908 *and 40 cm below the surface, the water potential and volumetric water content sensors.*

909

910
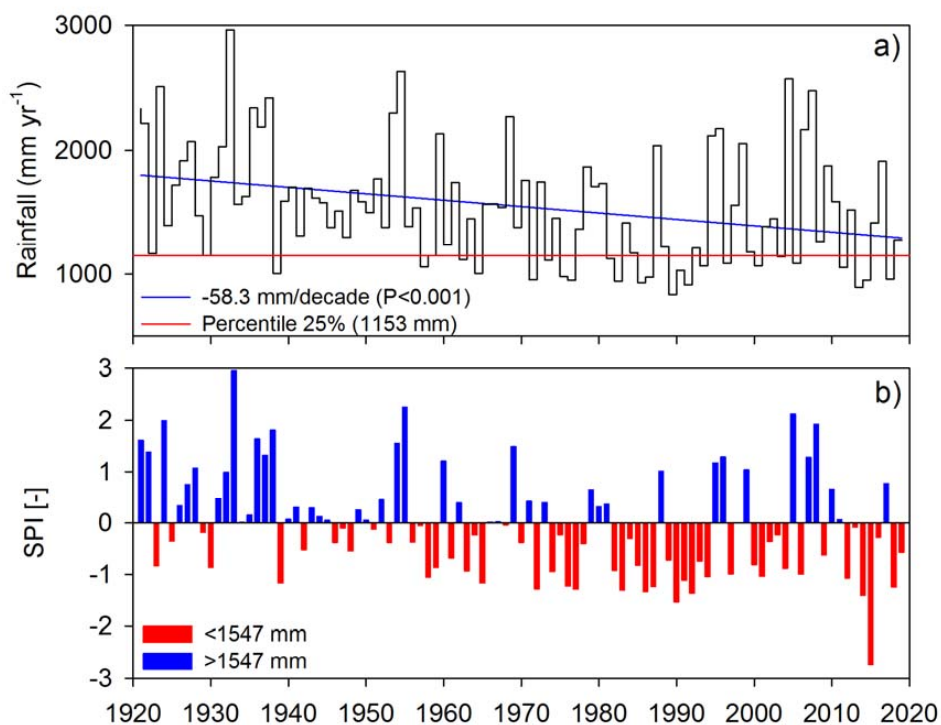
Figure 2   *(a) Long-term rainfall (mm yr⁻¹) including a significant rainfall decrease of -53 mm per decade (blue line) and 25% percentile of 1153 mm (red line as reference) and b) Standardized Precipitation Index (SPI) within the lowlands of Guanacaste between 1921-2019 (Long-term rainfall average=1547±473 mm yr⁻¹)(Rainfall data source: Ing. Werner Hagnauer, Cañas, Guanacaste).*
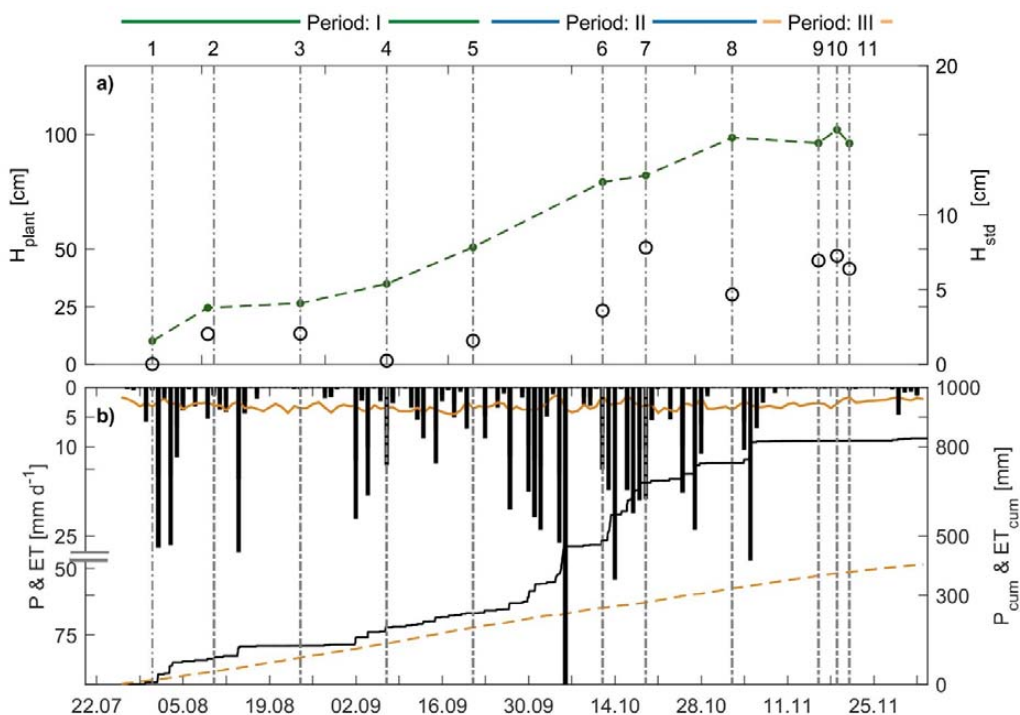
Figure 3   *Time series of (a) rice plant average height (H_{plant}) of the rice plants (filled green circles and dashed line) and the standard deviation the plant height (open black circles); b) precipitation (P, black bars), estimated evapotranspiration (ET, solid orange line), accumulated P (solid black line) and accumulated ET (orange dashed line). The different water sampling days 1-11 are indicated in each panel as vertical dashed lines and numbered on top of panel a and the date are given on the x-axis of panel b as dd.mm. Period I, II and III are indicated on the top of panel c.*

922
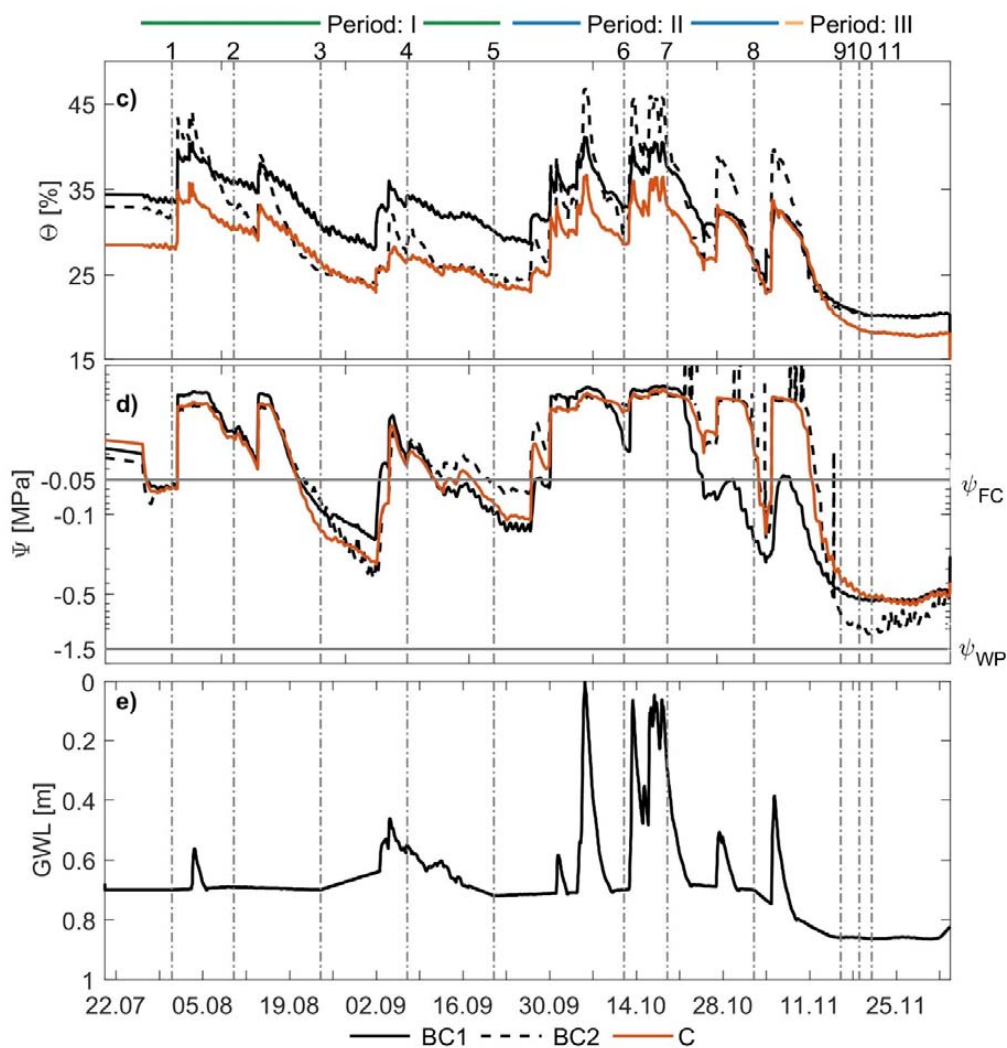
Figure 3   (continued) Time series of: (c) average volumetric water content and (d) the average water potential for each
treatment; (e) measured groundwater level. The different water sampling days 1-11 are indicated in each panel
as vertical dashed lines and numbered on top of panel c and the date are given on the x-axis of panel e as
dd.mm. Period I, II and III are indicated on the top of panel c.

Hydrology and
Earth System
Sciences
Discussions

Open Access

EGU
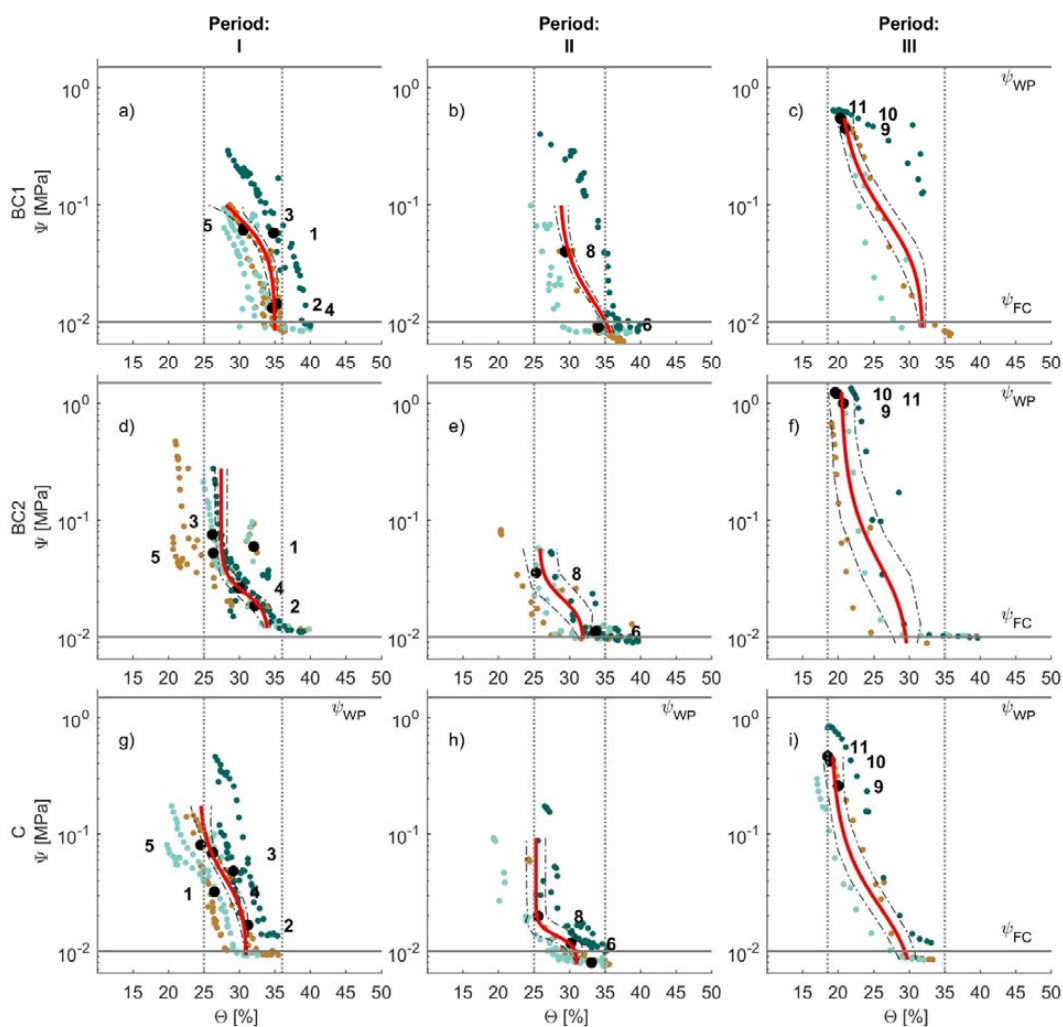
928   *Figure 4   The soil matric potential represented as a function of average soil water content of the different plots (colors)*
929   *for the treatments BC1 (a-c), BC2 (d-f) and C (g-i) and the Periods I, II and III (columns). The fitted average*
930   *soil water retention curves within a treatment using equation 1 (red line) including the 95% confidence interval*
931   *(dashed line). Black circles indicate the soil water content and soil matric potential on the sampling days*
932   *indicated by numbers.*

933
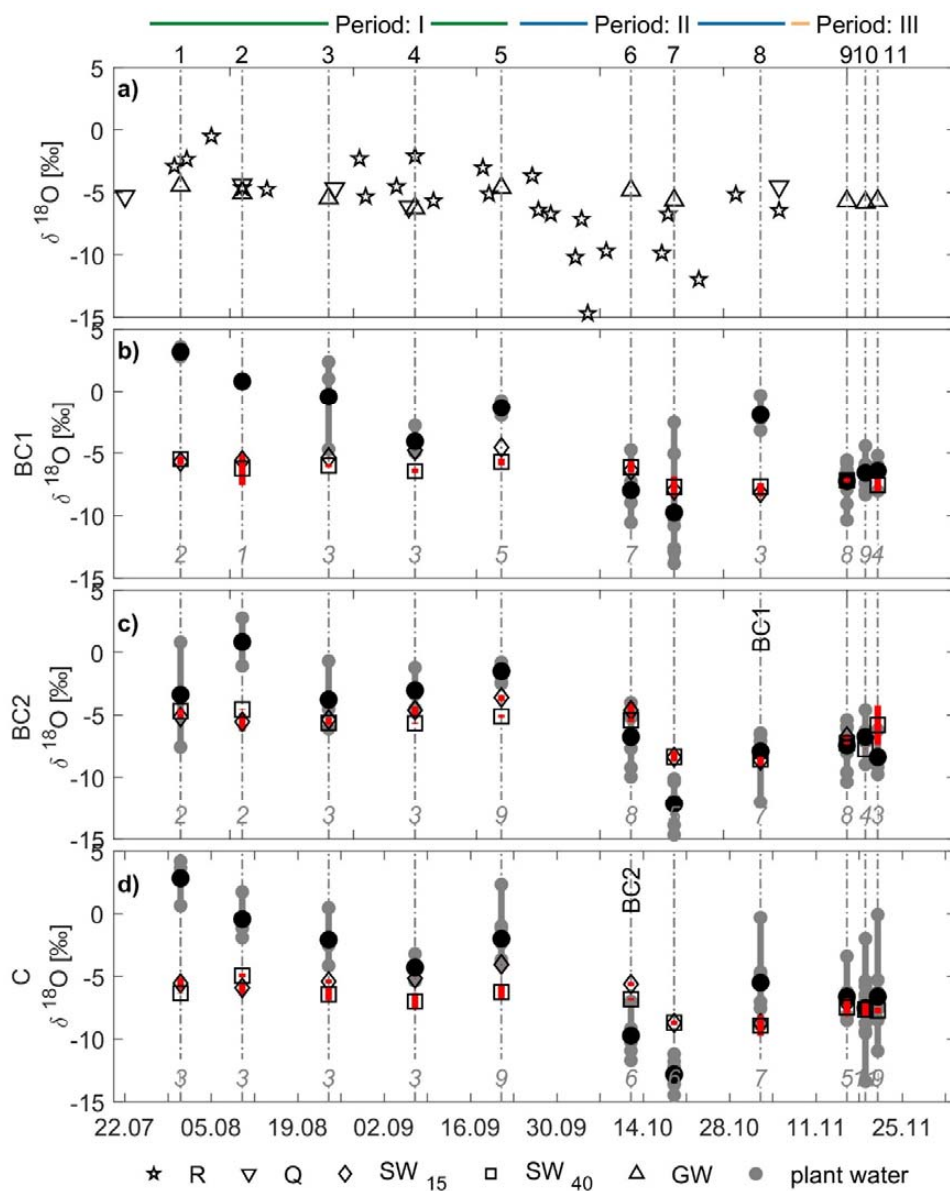
Figure 5 *Time series of (a) δ¹⁸O in rainfall, irrigation water, ground water and (b-d) soil water sampled at 15 cm (SW₁₅) and 40 cm (SW₄₀), ranges of δ¹⁸O of SW (red line). The δ¹⁸O of plant water (grey circle) and its average (black circle) are shown for the BC1 (b), BC2 (c) and control treatment (d), for sampling days 1-11 (indicated in each panel as vertical dashed lines and numbered on top of panel a). Period I, II and III are indicated on the top of panel a. Italic numbers in panels b-d indicate the numbers of plants samples. Significant differences among the average plant water values (per treatment n>3) of each sampling day are on the vertical dashed lines as letter of the treatment e.g. BC1, BC2 or C (Tukey's honestly significant difference criterion α = 0.05).*

Hydrology and
Earth System
Sciences
Open Access
Discussions
EGU

941
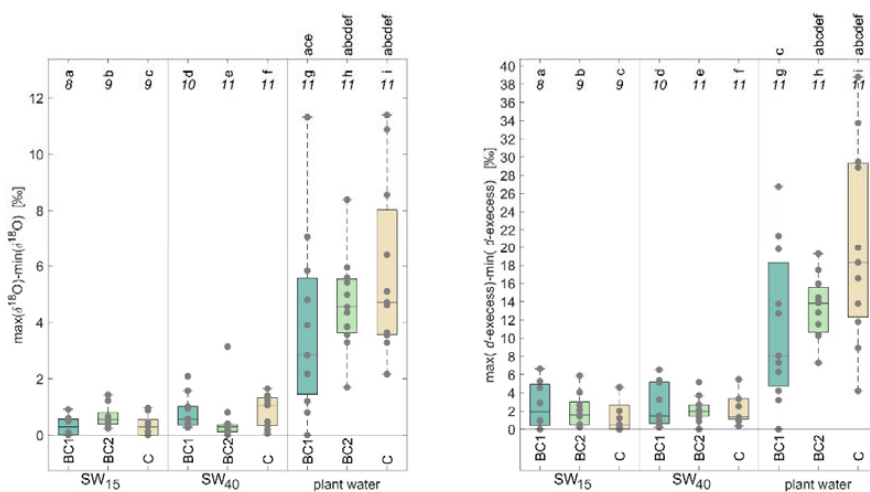
Figure 6 *The variability in stable isotope composition $\delta^{18}O$ (left) and d-excess (right) expressed as range (maximum-minimum observed isotopic composition) for the soil water collected at 15 cm (SW$_{15}$) and 40 cm (SW$_{40}$) below surface, and plant water in the BC1, BC2 and control treatment. The boxes show the range of values for different sample groups (showing the median and the interquartile range, with whiskers indicating 10th and 90th percentiles). Circles indicate the data points. Numbers above each box indicate the number of samples available. Letters on top of each box indicate significant differences among the average values of the different groups (Tukey's honestly significant difference criterion α = 0.05).*

949
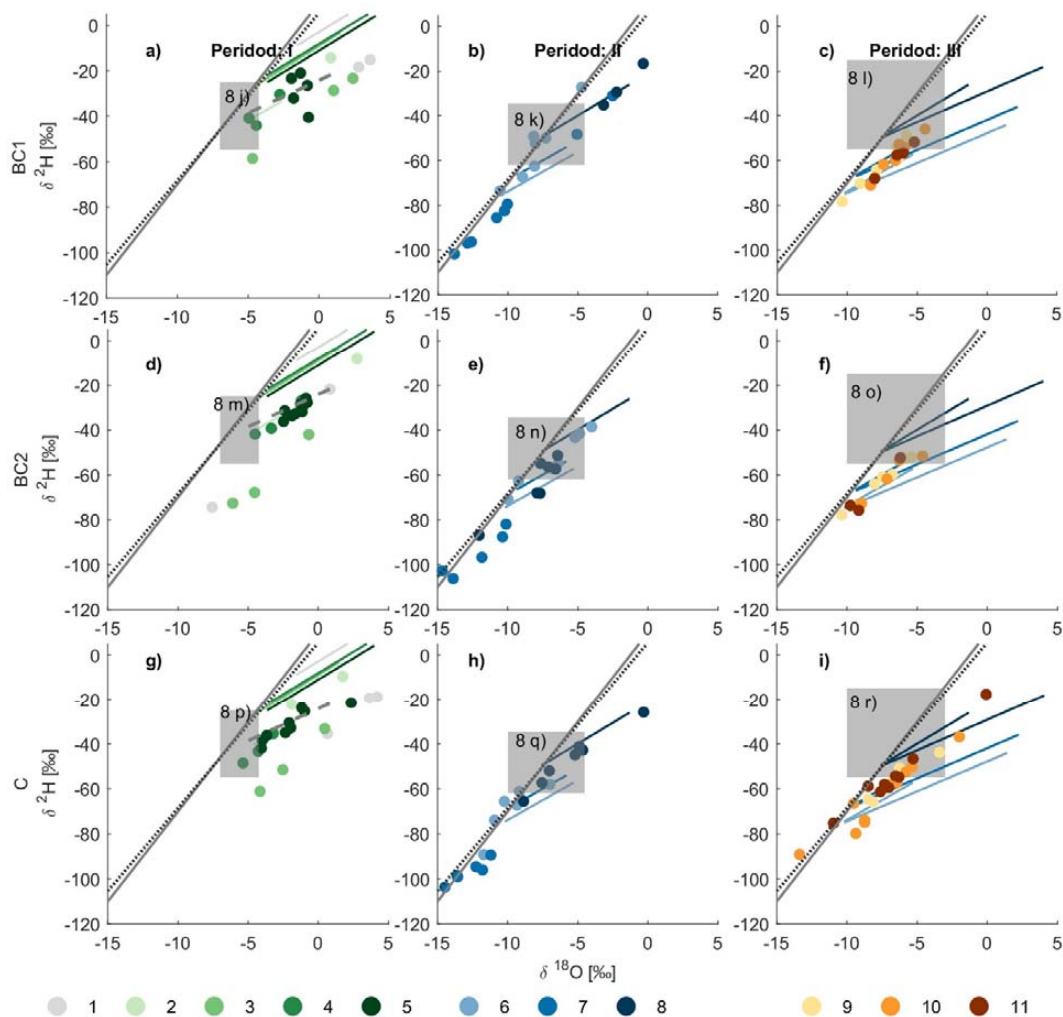
Figure 7 The dual isotope space with the isotopic composition of plant water samples (circles), the calculated evaporation lines of residual rainfall and sampled soil water for the treatments BC1 (a-c), BC2 (d-f) and C (g-i) and periods I-III (columns). Colors indicate the different sampling days (note that lines in period III are blue because they have been obtained from samples taken in period II). The local meteoric line (black dotted line) and global meteoric water line (grey solid line) are indicated in all panels. The grey dashed lines (panel a, d and g) indicate the evaporation line of median soil water. Isotopic compositions of irrigation, soil water and groundwater vary within the grey shaded squares indicated as 8 j-8 r, and enlarged in figure 8 j-r.

Hydrology and
Earth System
Sciences
Open Access
Discussions
EGU

958
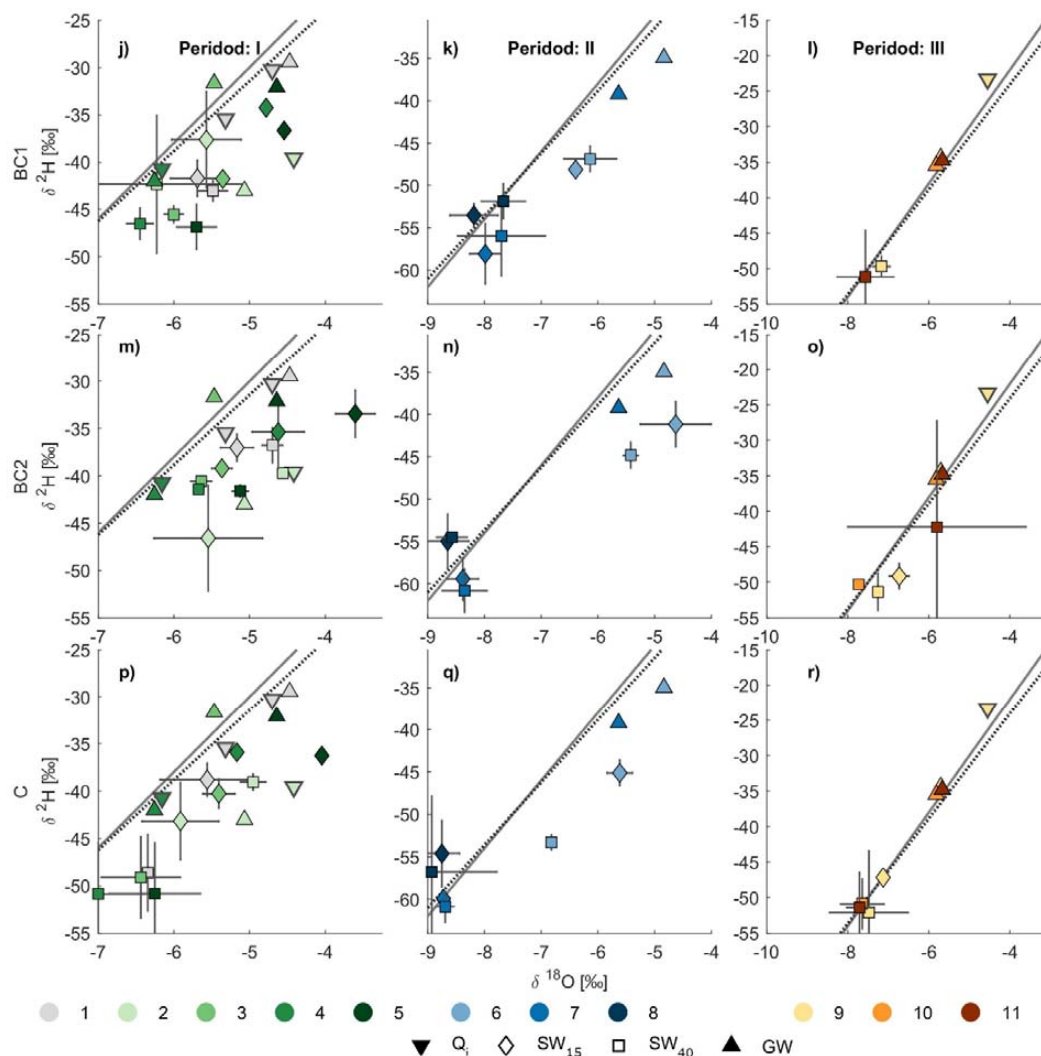
Figure 8   The dual isotope space with the isotopic composition of irrigation (down facing triangle), soil water collected at
15 cm (SW$_{15}$, diamond) and 40 cm (SW$_{40}$, square) and groundwater (upward facing triangle). The local
meteoric line (black dotted line) and global meteoric water line (grey solid line) are indicated in all panels. The
different treatments BC1 (j-l), BC2 (m-o) and C (p-r) and different periods I-III (columns) indicated in grey
panels of Figure 7 a-i. Colors indicate the different sampling days.

Hydrology and
Earth System
Sciences
Discussions

Open Access

EGU

964   # Appendix

965   *Table A1   Soil characteristics of the experimental site.*

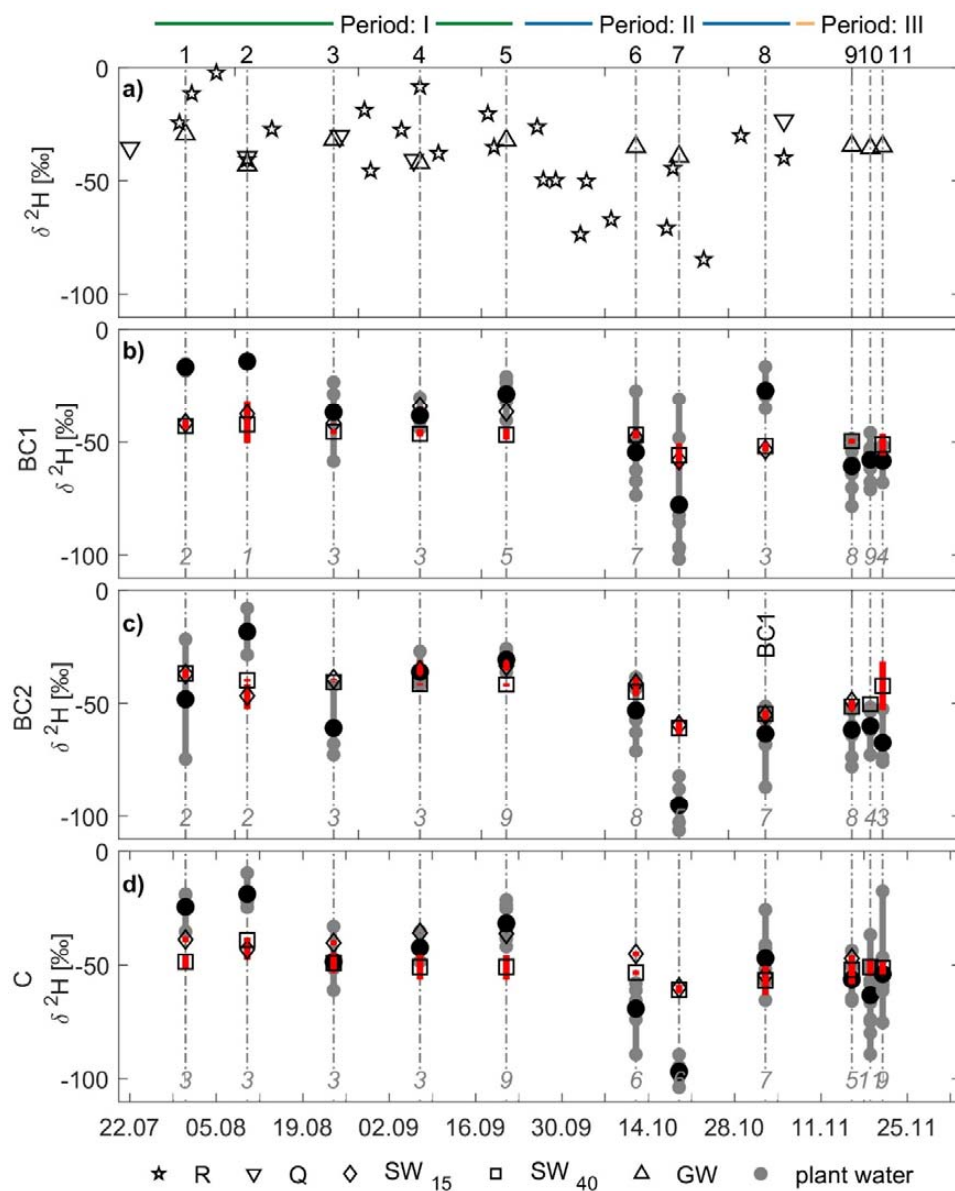|	BC1	BC2	C
Soil (0-20 cm) texture sand/silt/clay	34/30/36		
Infiltration capacity Wet / Dry season [mm h^{-1}]	15 / 30	15 / 40	8/40
pH	6.5	6.3	6.4
Ca [mol kg-1]	11.77	12.43	11.77
Mg [mol kg^{-1}]	2.60	2.63	2.47
K [mol kg^{-1}]	0.87	0.97	0.80
P [mg L^{-1}]	22.3	29.0	21.6
Zn [mg L^{-1}]	3.2	3.3	3.1
Mn [mg L^{-1}]	24.0	30.6	22.0
Cu [mg L^{-1}]	9.3	11.0	9.6
Fe [mg L^{-1}]	43.00	57.33	45.00
Organic C [%]	2.29	2.18	2.16
Total N [%]	0.15		

966

967

968 ***Table A2*** ***The fitted parameters θ_r, α and n the average soil water retention curves of the different treatments (BC1, BC2***
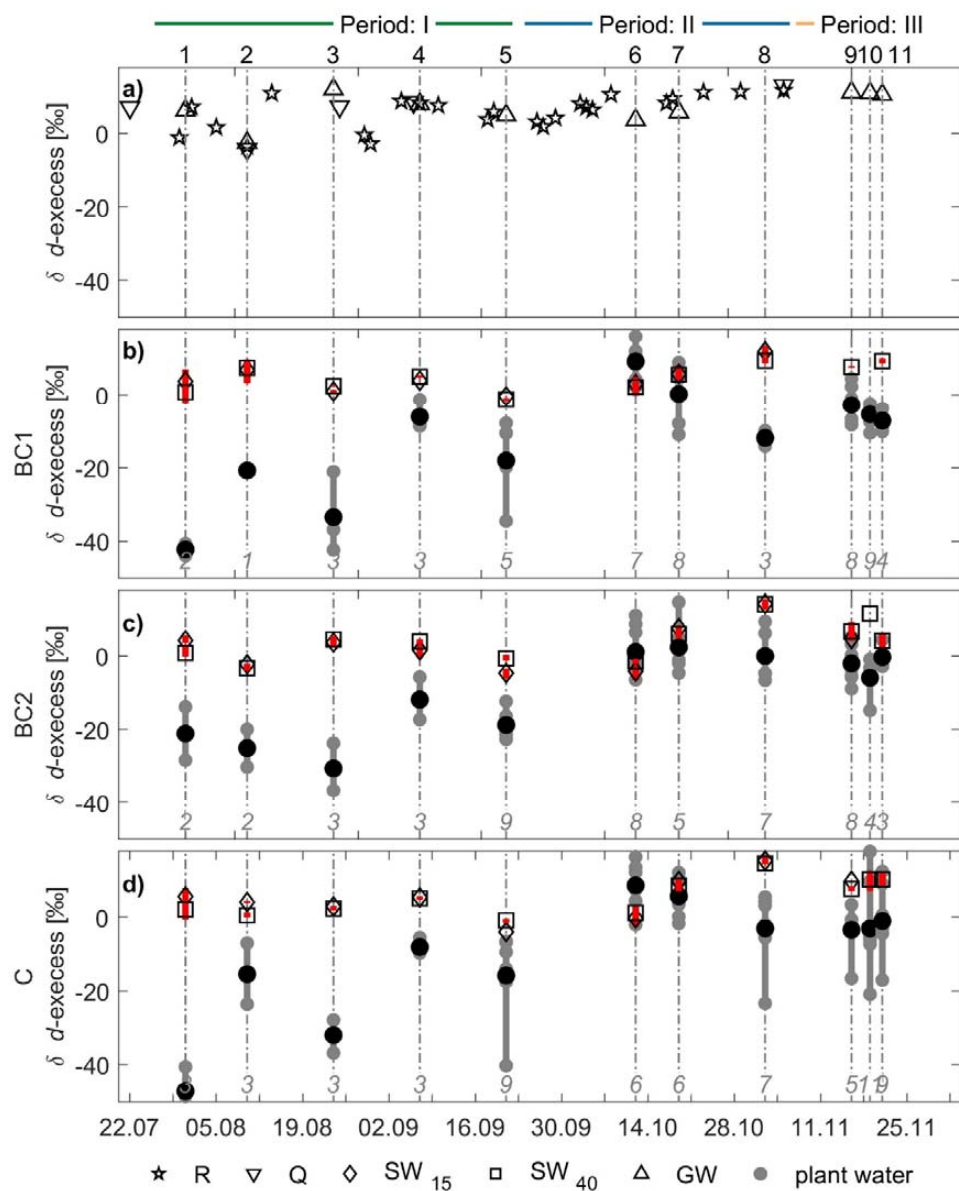969 ***and C) and the Periods I-III of equation 1 with the 95% confidence interval in brackets.***

|	BC1			BC2			C		
	Period			Period			Period		
	I	II	III	I	II	III	I	II	III
θ_r	0.2	0.3	0.2	0.3	0.3	0.2	0.2	0.3	0.2
	(-0.2,0.6)	(0.3,0.3)	(0.2,0.2)	(0.3,0.3)	(0.2,0.3)	(0.2,0.2)	(0.2,0.3)	(0.2,0.3)	(0.2,0.2)
α	13	78	18	44	49	34	27	75	58
	(-6.7,33)	(65,90)	(8.1,29)	(36,52)	(29,70)	(-14,81)	(20,34)	(61,88)	(30,85)
n	2.5	2.6	2	5.7	5.1	2	3	10	2
	(-0.3,5.4)	(1.8,3.4)	(0.9,3.1)	(1.4,10)	(-0.2,12)	(0.2,3.8)	(1.2,4.8)	(-0.4,24)	(1.2,2.9)

970

Figure A1 *Time series of (a) δ^2H in rainfall, irrigation water, ground water and (b-d) soil water sampled at 15 cm (SW15) and 40 cm (SW40), ranges of δ^2H of SW (red line). The δ^2H of plant water (grey circle) and its average (black circle) are shown for the BC1 (b), BC2 (c) and control treatment (d), for sampling days 1-11 (indicated in each panel as vertical dashed lines and numbered on top of panel a). Periods I, II and III are indicated on the top of panel a. Italic numbers in panels b-d indicate the numbers of plants samples. Significant differences among the average plant water values (per treatment n>3) of each sampling day are on the vertical dashed lines as letter of the treatment e.g. BC1, BC2 or C (Tukey's honestly significant difference criterion $\alpha = 0.05$).*

979

Figure A2 *Time series of (a) d-excess in rainfall, irrigation water, ground water and (b-d) soil water sampled at 15 cm (SW$_{15}$) and 40 cm (SW$_{40}$), ranges of d-excess of SW (red line). The d-excess of plant water (grey circle) and its average (black circle) are shown for the BC1 (b), BC2 (c) and control treatment (d), for sampling days 1-11 (indicated in each panel as vertical dashed lines and numbered on top of panel a). Periods I, II and III are indicated on the top of panel a. Italic numbers in panels b-d indicate the numbers of plants samples. Significant differences among the average plant water values (per treatment n>3) of each sampling day are on the vertical dashed lines as letter of the treatment e.g. BC1, BC2 or C (Tukey's honestly significant difference criterion α = 0.05). The d-excess was defined as d-excess = $\delta^2H - 8 \cdot \delta^{18}O$ (Dansgaard, 1964) using data from Figure 5 and A1.*

Hydrology and
Earth System
Sciences
Open Access
Discussions
EGU

989
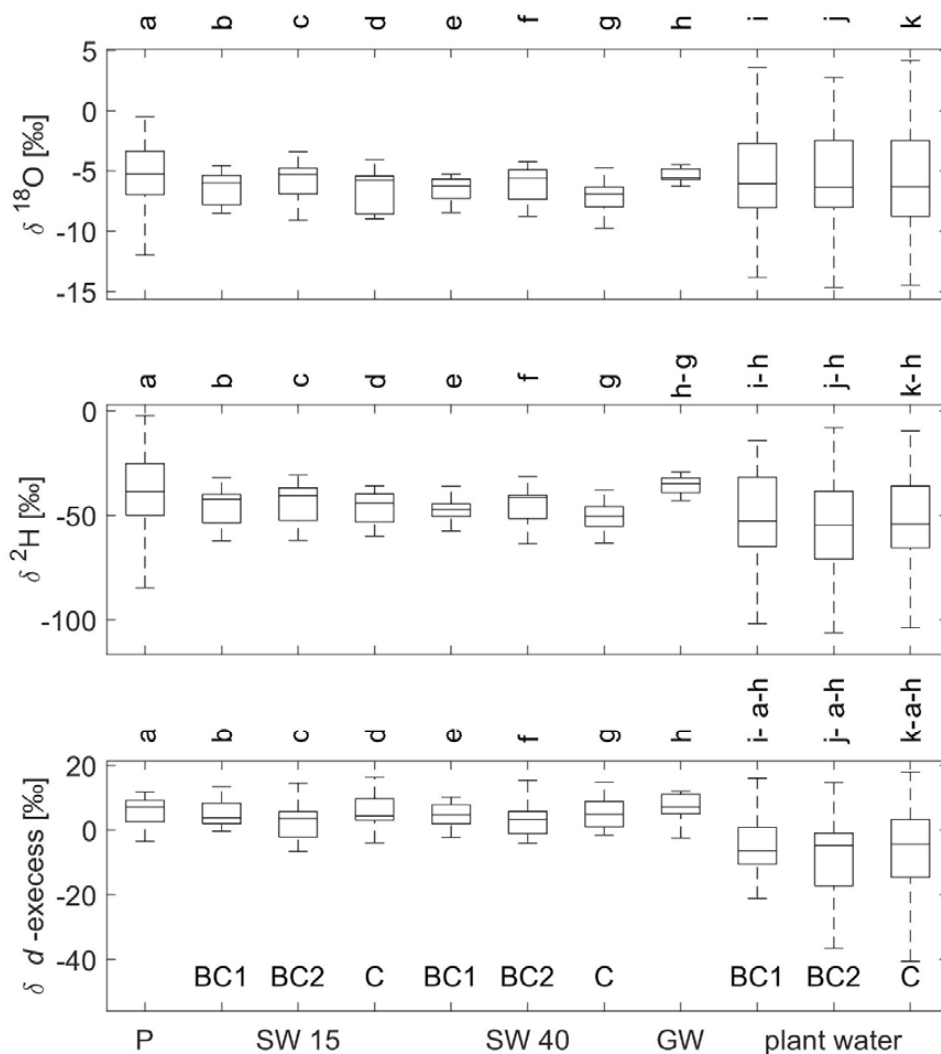
Figure A3 *The variability in stable isotope composition $\delta^{18}O$, δ^2H and d-excess. The x-axis indicates the sampled precipitation, soil water collected at 15 cm (SW$_{15}$) and 40 cm (SW$_{40}$) below surface, groundwater and plant water where BC1, BC2 and C indicate the three different treatments. The boxes show the range of values for different sample groups (showing the median and the interquartile range, with whiskers indicating 10th and 90th percentiles). Letters on top of each box indicate significant differences among the average values of the different groups (Tukey's honestly significant difference criterion α = 0.05).*